

Report No. 75305

Q

3  
10  
45  
0  
AD A1203  
**FEASIBILITY ASSESSMENT OF THE  
PERFUSION SCREEN CAMOUFLAGE CONCEPT**

Robert E. Wallace  
Vaughn J. Koester  
William E. Volz  
Varo, Inc.  
Integrated Systems Division  
2201 W. Walnut St.  
Garland, Texas 75040

May, 1982

Final Report

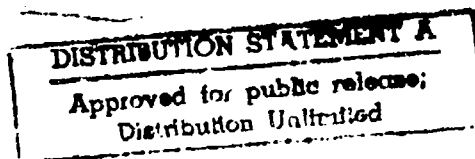


Distribution of this report is unlimited

FILE COPY  
FILE  
DRDME

Prepared for:

U.S. Army Mobility Equipment Research  
and Development Command  
ATTN: DRDME-RT  
Fort Belvoir, Virginia 22060



82 10 20 040

The views, opinions, and/or findings contained in the report are those of the authors and should not be construed as an official Department of the Army position, policy, or decision, unless so designated by other documentation.

Report No. 75305

FEASIBILITY ASSESSMENT OF THE  
PERFUSION SCREEN CAMOUFLAGE CONCEPT

Robert E. Wallace  
Vaughn J. Koester  
William B. Volz

Varo, Inc.  
Integrated Systems Division  
2201 W. Walnut St.  
Garland, Texas 75040

May, 1982

Final Report

Distribution of this report is unlimited

Prepared for:

U.S. Army Mobility Equipment Research  
and Development Command  
ATTN: DRDME-RT  
Fort Belvoir, Virginia 22060



## UNCLASSIFIED

SECURITY CLASSIFICATION OF THIS PAGE (When Data Entered)

REPORT DOCUMENTATION PAGE		READ INSTRUCTIONS BEFORE COMPLETING FORM
1. REPORT NUMBER	2. GOVT ACCESSION NO.	3. RECIPIENT'S CATALOG NUMBER
	AD-A120 553	
4. TITLE (and Subtitle) FEASIBILITY ASSESSMENT OF THE PERFUSION SCREEN CAMOUFLAGE CONCEPT	5. TYPE OF REPORT & PERIOD COVERED Final	
6. AUTHOR(s) Robert E. Wallace Vaughn J. Koester William B. Volz	7. PERFORMING ORG. REPORT NUMBER 75305	
8. PERFORMING ORGANIZATION NAME AND ADDRESS Varo, Inc., Integrated Systems Division 2201 W. Walnut Street Garland, Texas 75040	9. CONTRACT OR GRANT NUMBER(S) DAAK70-81-C-0221	
10. CONTROLLING OFFICE NAME AND ADDRESS USA MERADCOM, ATTN: DRDME-RT Fort Belvoir, VA 22060	11. REPORT DATE May , 1982	
12. MONITORING AGENCY NAME & ADDRESS (if any, other than Controlling Office)	13. NUMBER OF PAGES 134	
	14. SECURITY CLASS. (of this report) UNCLASSIFIED	
	15. DECLASSIFICATION/DOWNGRADING SCHEDULE	
16. DISTRIBUTION STATEMENT (of this Report)  Distribution of this report is unlimited.		
17. DISTRIBUTION STATEMENT (for the abstract entered in Block 20, if different from Report)		
18. SUPPLEMENTARY NOTES		
19. KEY WORDS (Continue on reverse side if necessary and identify by block number) camouflage infrared thermal		
20. ABSTRACT (Continue on reverse side if necessary and identify by block number) This study examines the feasibility of the perfusion screen camouflage concept primarily as thermal infrared camouflage, but also in regard to its potential as a component of the CS-86 universal camouflage system. Thermal performance criteria were developed. A two layer form of perfusion screen was developed and tested. Results indicate feasibility as thermal camouflage and compatibility with CS-86 requirements.		

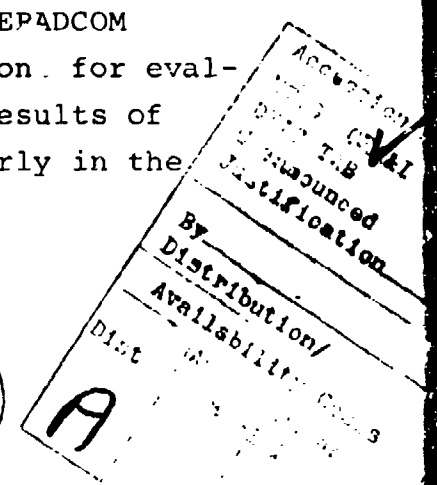
## SUMMARY

This contract was directed at an evaluation of the perfusion canopy concept for thermal suppression. This concept concerns thermal camouflage which provides for the perfusion of air through the canopy to enhance convective coupling to air temperature. In conjunction with openness to air passage, the canopy still maintains a complete line-of-sight block so that the canopy becomes a barrier to direct view of any part of an object behind it.

By means of air perfusion it was anticipated that solar load could be dissipated without canopy temperatures which are in excess of those occurring in the background. In the same way, the influence of night cooling to the cold sky was expected to be diminished. Both solar induced overheating and nighttime overcooling were problems which have been experienced with insulating blankets used for thermal camouflage.

More specifically, the goal of this contract was to develop and evaluate the perfusion canopy concept for thermal suppression as a component of the Modular Multi-Spectral Camouflage System 1986 (CS-86).

Attention was first directed to defining a working requirement for what thermal suppression should be and what thermal loads would be anticipated. This task was performed independently by Varo, without MERADCOM inputs, in order to establish working definition for evaluation of perfusion canopy performance. The results of this effort were concurred with by MERADCOM early in the program, and are displayed in Addenda 1 and 2.



Structural analysis was carried out to find the type of incising which could be used and determine factors controlling line-of-sight blocking. It was found, in fact, that only two layers are essential to achieve 100% blocking. Based on what structural analysis showed, half meter square samples were prepared for testing. A thermal equation was also set up describing the heat balance in the perfusion canopy.

Testing took place in two phases: preliminary radiometric temperature tests and then imaging tests in which an actual 8-12  $\mu\text{m}$  imager was used to view the three samples outdoors under a variety of conditions.

The perfusion screens did cope with solar load so that they remained within the background radiant variation when there was a clear sky. When the cloud cover was high, yet the sun still was able to strike the samples, they were more likely to rise above the background radiant variation slightly. They were in all day tests much cooler than a thermal blanket section. At night, the perfusion screens did not overcool as was the case for thermal blankets.

Some experimentation with a hot plate behind the screens shows that they are indeed thermally opaque (do not transmit direct infrared energy). A spacing of about six inches was also found to be sufficient for the test condition to reduce the influence of the hot plate on screen radiance to an insignificant level.

The present development and evaluation has indicated, therefore, that the perfusion canopy concept offers a viable means to achieve thermal concealment in solar load conditions and at night when overcooling is a problem for insulative blankets. It was also concluded that this concept is compatible with implementation of camouflage in other wavelength regions. Further development was recommended.

## PREFACE

Work performed in this development/study was authorized under Contract DAAK70-81-C-0221 from the Mobility Equipment Research and Development Command (MERADCOM) at Fort Belvoir, Virginia. The effort was directed at the development and evaluation of the perfusion canopy concept for thermal suppression as a component of the Modular Multi-spectral Camouflage System 1986 (CS-86).

The authors wish to acknowledge the assistance and advice of Mr. Henry Atkinson of MERADCOM.

## CONTENTS

	<u>Page</u>
SUMMARY	1
PREFACE	3
CONTENTS	4
1.0 INTRODUCTION	7
2.0 INVESTIGATION	9
2.1 Requirements for thermal suppression and thermal load.	9
2.2 Material selection.	11
2.3 Structural analysis.	13
2.3.1 Slit geometry considerations.	17
2.4 Tests of the perfusion screen	28
2.4.1 Radiometric temperature testing.	29
2.4.1.1 Results of radiometric temperature testing.	33
2.4.1.2 Conclusion from radiometric temperature tests.	37
2.4.2 Imaging tests.	38
2.4.2.1 Imaging tests description.	39
2.4.2.2 Imaging test results.	40
2.4.2.3 Imaging tests conclusions.	53
2.5 Thermal equation for the perfusion screen.	58
2.5.1 Heat balance equation.	58
2.5.2 Radiation terms.	59
2.5.3 Convection term.	60
2.5.3.1 Idealized convection equations.	60
2.5.3.2 Determination of significant length.	63
2.5.3.3 Perfusion screen convection model.	63
2.5.4 Energy balance result.	65
2.5.5 Energy balance calculation for obtaining perfusion factor.	68

CONTENTS (CONTINUED)

	<u>Page</u>
3.0 DISCUSSION.	75
3.1 CS-86 compatibility.	75
3.2 Difficulties of the perfusion screen.	78
3.3 Surface garnishment.	80
4.0 CONCLUSIONS.	81
4.1 Thermal suppression requirements and thermal load.	81
4.2 Thermal suppression performance.	82
4.2.1 Night performance	82
4.2.2 Day performance	83
4.2.3 Miscellaneous conclusion.	84
4.3 CS-86 component viability.	84
5.0 RECOMMENDATIONS.	87
REFERENCES	90
APPENDIX A. Actual Temperature from Radiometric Blackbody Temperature (Measured with R2LT)	91
APPENDIX B. Radiometric Measurement of Air Temperature	95
APPENDIX C. Assessment of Effective Blackbody Temperature of Sky and Solar Absorptance for Forest Green Paint	99
APPENDIX D. Emissivity Measurement on Forest Green Paint	107
APPENDIX E. Infrared Imager Specifications	109
ADDENDUM 1	111
ADDENDUM 2	137

## 1.0 INTRODUCTION

The purpose of this contract was to develop and evaluate a new concept for thermal camouflage to assess its potential for thermal suppression and its applicability as a component of the Modular Multi-Spectral Camouflage System 1986 (CS-86). The concept has been called the "perfusion screen" or "perfusion canopy". This is an idea originated at Varo\* on which a limited amount of testing had been done, which indicated the likelihood that a perfusion screen could respond to both solar loading and night-time cooling in a manner similar to the behavior of foliage under the same conditions.

Prior thermal blankets suffer from the disadvantage of too great a response to radiative effects of the environment. Because they are large flat type surfaces, both solar heating in the day and cooling to the cold night sky are thermal forces which have more than desirable influence on blankets. Therefore, blankets can become either too warm or too cold in response to different environments.

The perfusion screen concept is one which is aimed at increasing convection effects relative to radiative heating or cooling so that the screen temperature is more strongly coupled to air temperature. Thus radiative effects are muted. At the same time, however, the screen must not allow an observer using a thermal viewer to see directly through the screen because the hidden object (which the screen is intended to camouflage) is actually a source and not merely a reflector of light which is the case in the visual spectrum. If it were not substantially thermally opaque, the screen on a hot target would be the thermal equivalent of lace on a light bulb visually. Radiant energy would be attenuated somewhat but the leakage would still be quite adequate to permit detection.

---

\* Patent applied for, serial number 308,134

The perfusion screen is a type of barrier which prevents a direct view of objects behind the screen, yet is open to passage of air through the screen (perfusion of air). It is this openness of air passage which accounts for its tendency to stay at temperatures close to air temperature. Because it is a screen barrier type of camouflage like the lightweight synthetic screen, it is possible that it can be configured to perform visual, near infrared, and radar camouflage function as the synthetic screen does. Thus it offers potential to combine in one system, camouflage for all anticipated wavebands. That is the goal of the CS-86 system; thus, this contract was undertaken to evaluate the concept as a component of the CS-86 system.

The problem of this contract for assessment of the applicability of the perfusion screen concept to CS-86 was broken into two parts: development and evaluation of thermal suppression capability of the perfusion screen and an evaluation of the compatibility of the perfusion screen to visual, radar, and near infrared concealment tasks. Most emphasis was placed on thermal suppression capability - namely to see if this approach can deal effectively with the problems of solar heating in the day and night sky overcooling experienced by thermal blankets.

As a first step in thermal suppression assessment, before any perfusion screen design, evaluation or testing was done, considerable attention was given to determination of a working definition of a suppression requirement. It was to serve as a standard against which to measure thermal load imposed on the perfusion screen by hot targets over which the screen may be placed. The load was essentially taken to be determined, as far as the target is concerned, by target surface temperatures.

Once the requirement and expected thermal load was determined, a description was submitted to MERADCOM and was approved. The results are displayed in Addenda 1 & 2.

The design task for the perfusion screen was two pronged: empirical and theoretical. The empirical approach was used in study of candidate patterns of incising and layering of elements of the perfusion screen because of the difficulty of making theoretical predictions of bending and expansion results for slit sheets and of so determining thermal opacity of combinations. Therefore, small samples of candidate patterns were prepared and studied.

Theoretical analysis through the development of equations for the heat balance at an element of a perfusion screen was used both to aid in understanding the processes controlling temperature in a perfusion screen, and in predicting thermal results for screens when various parameters are varied and when a given screen is placed in a different environment from that in Texas.

Testing of sample perfusion screens in small size was performed initially through temperature measurement (blackbody temperature) radiometrically. After those test results had been analyzed, a thermal imager was rented to view the same screen samples and assess suppression performance more realistically.

## 2.0 INVESTIGATION

### 2.1 Requirements for Thermal Suppression and Thermal Load.

The first effort on this contract was to delve into the matter of forming an operating definition of the thermal suppression requirement and of thermal load seen by infrared camouflage. These investigations are detailed in Addenda 1 & 2. However, a summary of the conclusions from those addenda is given here.

The most exact thermal suppression requirement is the qualitative one that the equivalent blackbody temperature of the camouflage fall within the naturally occurring range of background blackbody temperatures. This may be too restrictive in the case of unresolved targets (point sources).

A more quantitative rule of thumb by which to assess thermal camouflage success is the goal that camouflage equivalent blackbody temperatures need to be within  $\pm 2$  to  $\pm 7^{\circ}\text{C}$  of average background, depending on environmental condition.

In regard to thermal patterning, it was decided that the smallest lobes in an irregular pattern should be on the order of 20 inches.

Angular coverage for thermal suppression should be the entire hemisphere strictly, but the analysis suggests that terrain masking may permit lack of thermal suppression in an angular region one to five degrees above the horizontal.

Thermal load for suppression considerations was regarded as either the typical target radiance difference with background (the job facing thermal camouflage), or as a measure of the influence of hot targets on temperature of thermal camouflage. In both cases, target surface temperature difference with ambient is the key. Rather sparse data yielded the following working definition of thermal load:

Daytime	30-40°C
Night	25-30°C

## 2.2 Material Selection.

Material selection was a necessary part of this effort but was not given a high priority as far as determining an optimum material for use with perfusion screens. The main concern was one of having materials compatible with the structural requirements imposed because of the basic camouflage requirement of line of sight blockage, or thermal opacity. In fact, paper, due to its ubiquitousness, was used frequently as a material for trying out incising patterns. It is also a candidate material if disposability becomes a requirement.

It is recognized that in future work on the perfusion screen concept more attention would be needed to select materials for a number of reasons. Coating requirements in regard to visual camouflage and resistance factors of all sorts (chemical and environmental such as solar exposure, water, oil,...) as well as cost would be concerns. If disposability of the screen is determined to be a desirable feature, then of course some trading off of resistance factors would have to be done against cost. In addition, durability and strength factors should be considered.

Here, however, only the properties of materials regarding structural forming and to some extent visual appearance were taken into account. Thus the material which is presently being used in the synthetic camouflage nets, a coated cloth, was experimented with because it already had the required visual coloration and so would approximate the expected solar absorption characteristics of the perfusion screen as it should be made.

It was noted in experimentation with different slit dimensions that this camouflage cloth behaved differently. Other materials experimented with were spunbonded polyolefin (paper-like plastic), polyester film, and Kraft paper already incised for a different purpose.

Polyester film is an interesting material because it has the property of taking a heat set. When deformed after once being set, it will spring back to the heat-set position when mechanical deformation force is released. It is, however, a fairly brittle material subject to tearing. In this application (sheet subdivided into a multiplicity of slits) every slit offers a potential tear spot. In spite of this disadvantage, polyester might still be considered for reusable camouflage because of its springiness and heat-setability. A polyester perfusion canopy set in the expanded state could probably be flattened and rolled up for compact storage. Then when next needed, it would automatically open properly when unrolled.

Spunbonded polyolefin material was chosen for making the test perfusion canopies for several reasons. It was available, it was readily slit, and the slits resisted tearing. It was also paintable and water resistant. Therefore, it served acceptably at the concept evaluation stage for testing perfusion canopy samples.

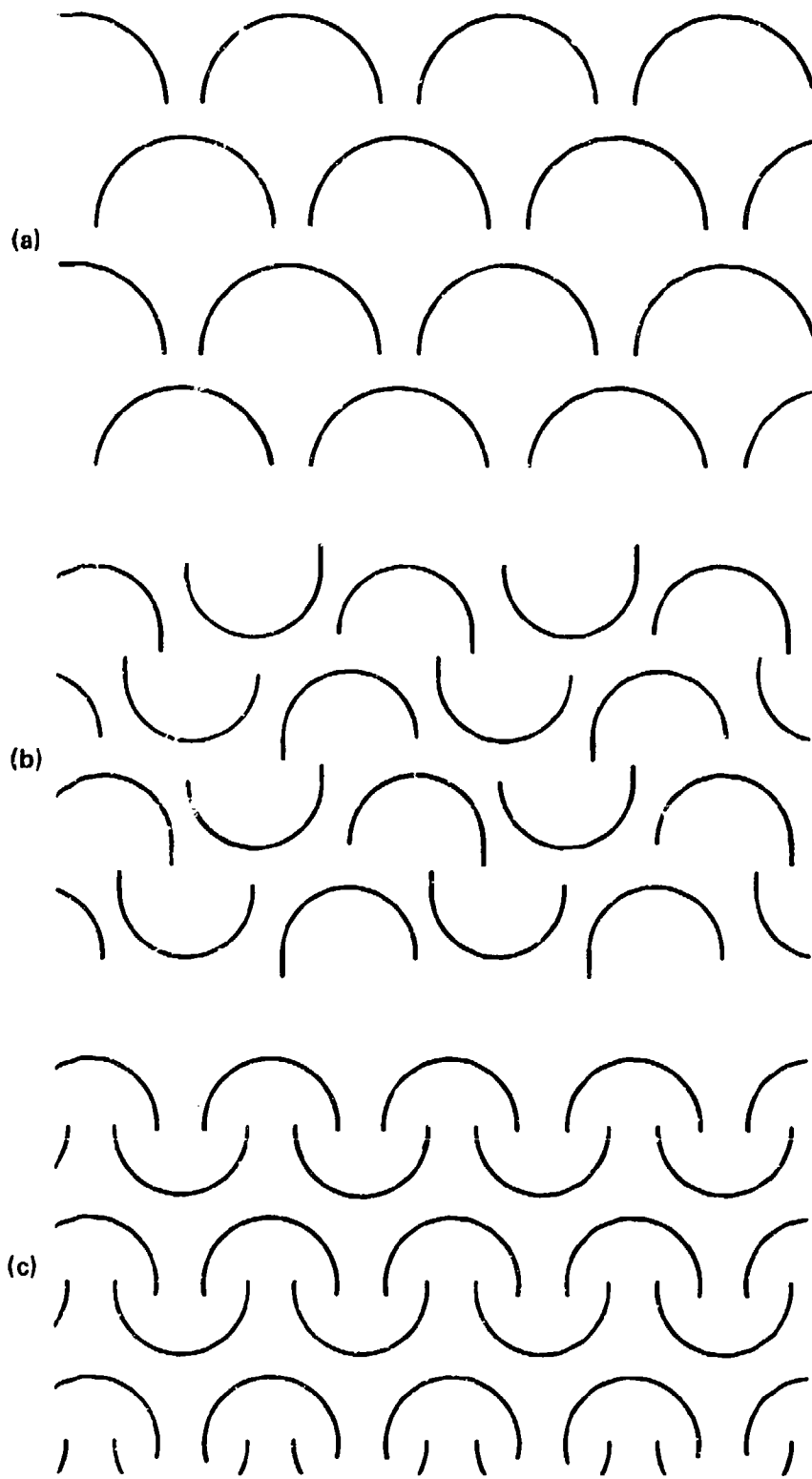
For coating the materials which were not already colored, a forest green paint described in MIL-E-52798A (ME) was picked. This paint was designed for infrared as well as visual reflectance. It is a dark appearing paint and it was selected because it probably affords a maximum solar absorptance which was regarded as a worst case for the perfusion screen thermal performance in the daytime.

### 2.3 Structural Analysis.

The purpose of structural analysis was to investigate methods of creating a line of sight barrier without preventing air flow through the screen. Exploration was made in the area of slit patterns first, trying to discover if there was any preferred geometry of slitting which would result in good blocking in conjunction with another sheet or sheets. It was also desired that the number of layers of slit expanded sheets be reduced to a minimum for reasons of costs, weight, complexity, handling and storage volume.

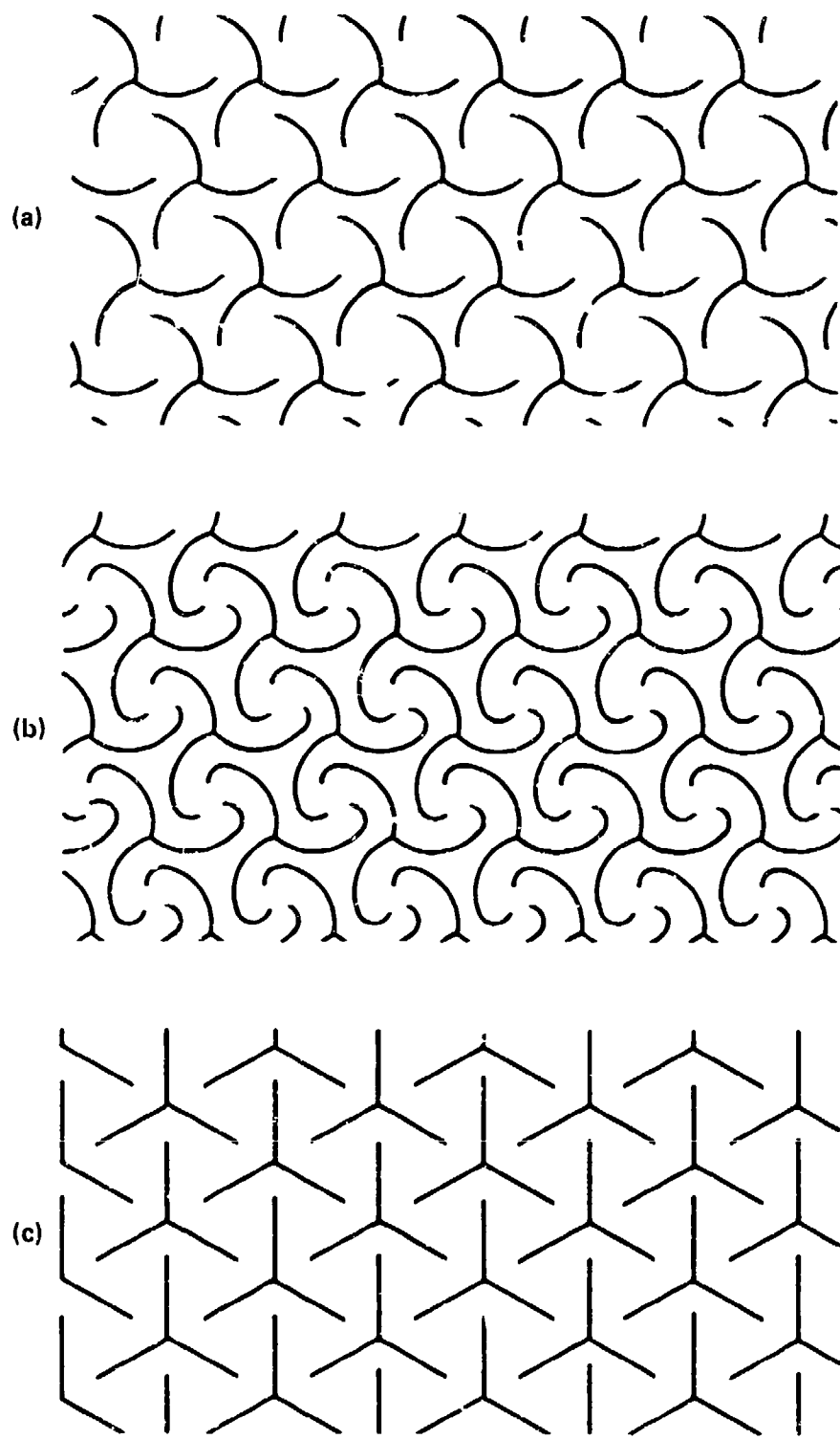
Since it was recognized at first that the theoretical treatment of slit sheet expansion, especially for curved slitting, would be intractible, the approach taken was to devise slitting designs and actually make paper samples of these patterns to physically examine the form of the slit openings when the sheet was opened. About nine different types of curved incising patterns were experimented with by preparing paper samples and trying out the expansion properties. Figures 1 through 3 show these patterns.

Among these are some which can be expanded by force along any line of expansion (Figure 2). That is because of the interlocking nature of the slit patterns on that figure. They seemed to afford easy expansion but not in an easily controllable way which would allow layer-to-layer registration. As both straight and curved slit patterns were experimented with, however, it became apparent that making the slits curved was not producing any advantage over a straight slit pattern in regard to line of sight blockage when patterns were layered together. Blocking, in fact, appeared to be more uncertain for the curved incising patterns than for the straight ones for the same number of layers. The straight slit pattern also had the



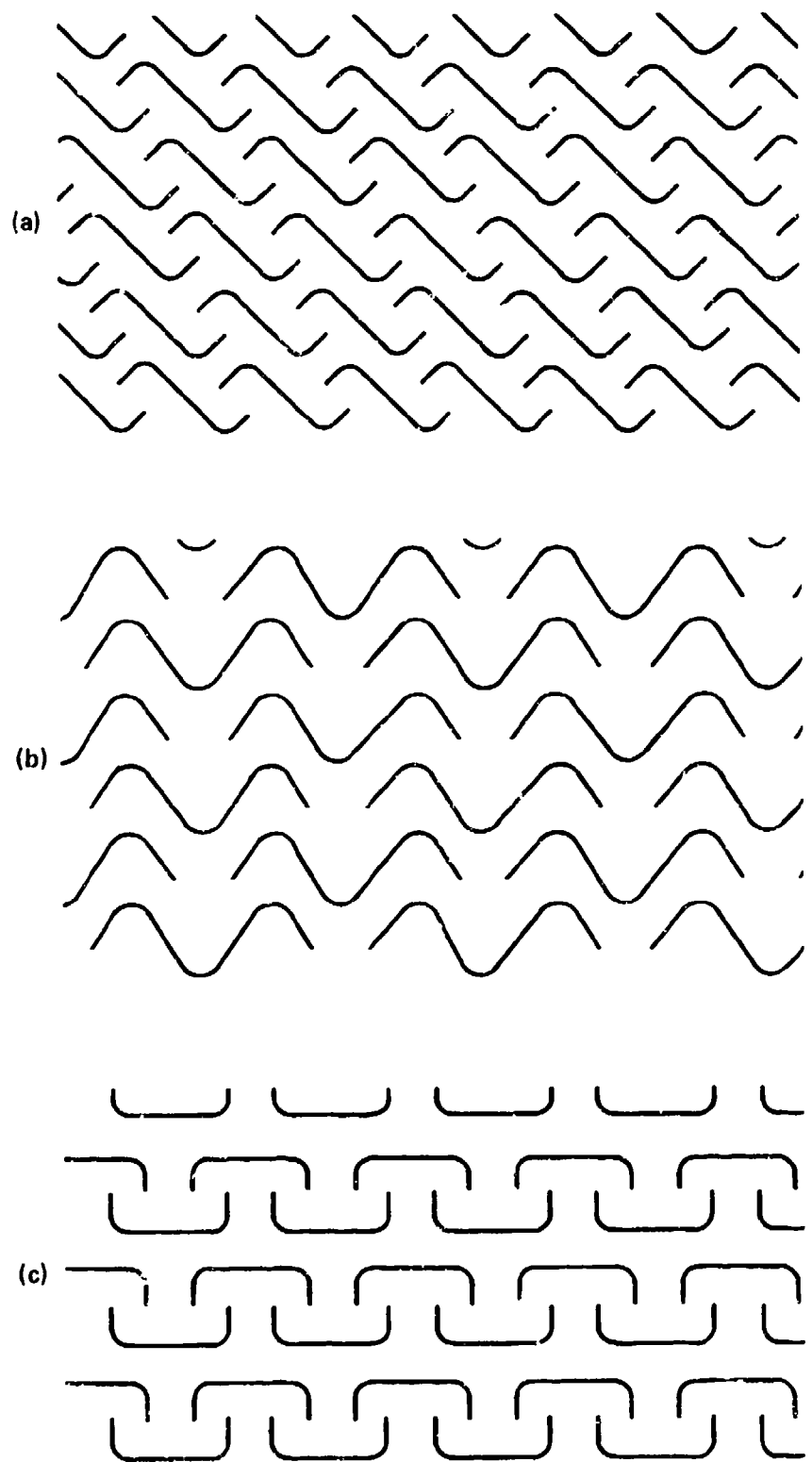
2195

Figure 1. Slit Patterns



2195

Figure 2. Slit Patterns



2195

Figure 3. Slit Patterns

advantage of easier producibility, thus curved patterns were abandoned in favor of straight.

Figure 4 shows some of the straight patterns tried. In that figure, significant dimensions  $s$ ,  $w$ , and  $d$  are defined. As these patterns were tried, it was noted that the ratio of  $s/d$  seemed to correlate with the stiffness of an expanded layer. For paper the ratio which was judged to afford the best stiffness for controllable slit openings (so that layers could be registered to create full blockage), was that for Figure 4 (b),  $s/d = 2$ . Two other factors which affect stiffness are material properties and the size of a slit pattern relative to material thickness. However, it was thought that a slit pattern dimension about like that in Figure 4 (b) would be suitable for a perfusion screen. Since paper-like material may be used, this geometry was selected. It was possible to align just two layers of this pattern so that no angle of observation would permit seeing through the layers yet sufficient openness was available to permit air passage.

A pattern such as that in Figure 4 (d) gives the impression of much greater springiness (less force to expand it); and it can also be registered to attain total blockage, but doing so was found to be more difficult than for pattern (b).

### 2.3.1 Slit Geometry Considerations.

The straight slit geometry for an expanded sheet has been examined to determine open area for perfusion of air and for blocking effects with a pair of expanded sheets. Figure 5 (a) shows the slit pattern in a flat sheet and 5 (b) gives the appearance of an expanded sheet isometrically. In Figure 5 (a) patterning defining dimensions  $w$ ,  $s$ , and  $d$  are shown.

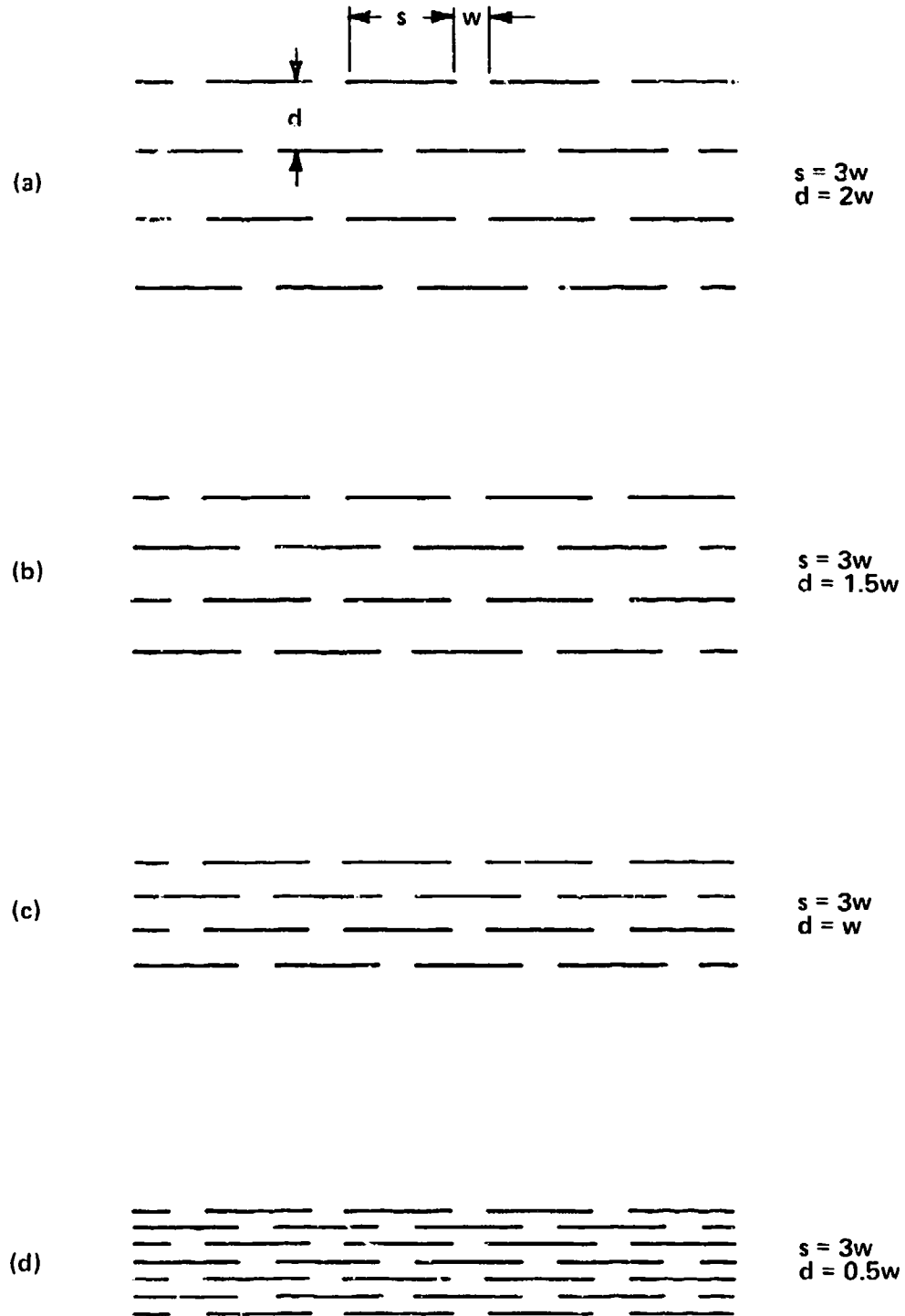
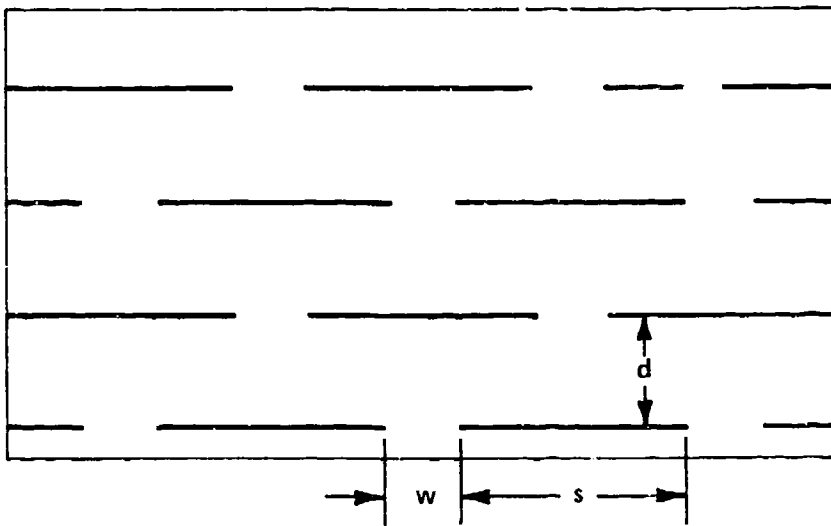
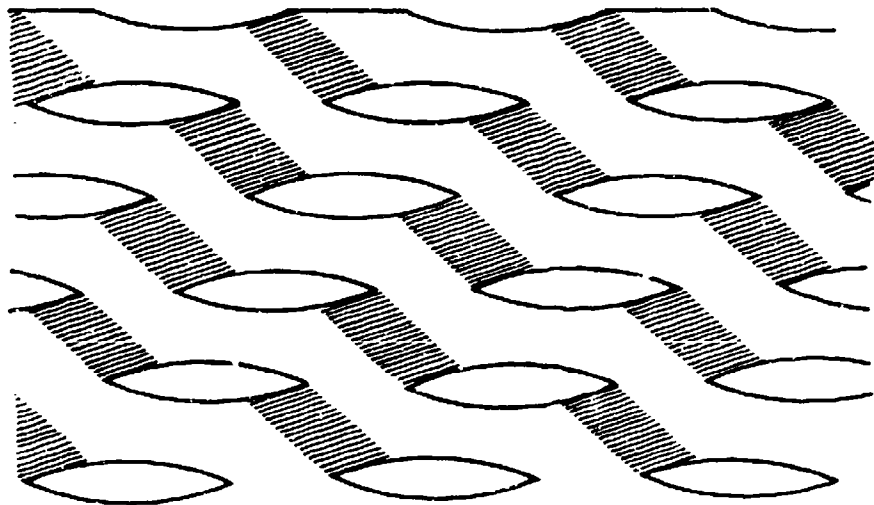


Figure 4. Straight Slit Patterns

2196



(a) FLAT PATTERN



2197

(b) EXPANDED SHEET

Figure 5. Geometry of Expanded Sheet with Straight Slitting

A side view of an expanded sheet is given in Figure 6 looking in a direction parallel to slit rows. The height of slit openings,  $h$ , depends on the expansion ratio  $R$ , defined as the expanded length divided by the unexpanded length. This ratio can be written using Figure 6 as

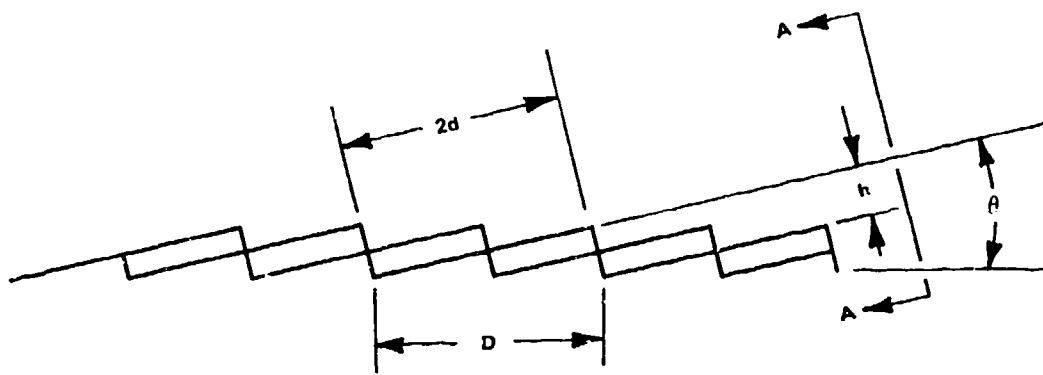
$$R = D/(2d) = 1/\cos \theta \quad (1)$$

One of the geometric aspects of an expanded sheet which is of interest from a perfusion flow standpoint is the open area ratio-i.e. the area of all the slit openings in an expanded sheet divided by the area of the expanded sheet. When the sheet is viewed from the direction of the arrows A-A in Figure 6, what is seen is a totally clear area obscured only by the edges of the material in a hexagonal pattern like chickenwire. This is the projected area of the sheet in that direction which is in the ratio  $h/D = \sin \theta$  to the total sheet area - i.e. the open area ratio is  $\sin \theta$  (ignoring for the moment any obscuration from the edges of the material). Combining this result with (1), the open ratio can be expressed as

$$A_o = \sin\left(\cos^{-1}(1/R)\right) \quad (2)$$

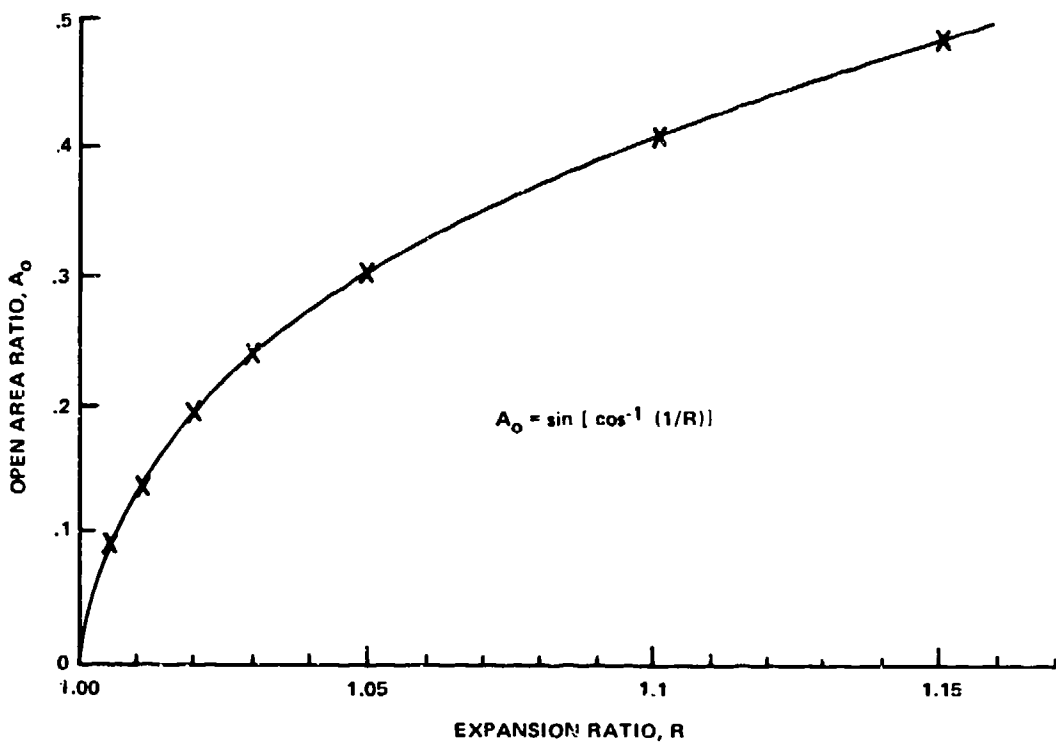
Figure 7 is a graph of the variation of open area ratio with the amount of expansion of a slit sheet. It is of interest to note that the expansion alone controls the open area ratio and not the relation between slit dimensions.

There is a small contribution to obscuration of the open area due to the edge area of slit openings. Figure 8 shows the appearance of an expanded sheet as viewed from the opening direction. The obscuration is approximated by the following development.



2198

Figure 6. Side View of Expanded Sheet in a Direction Parallel to Slit Rows



2199

Figure 7. Variation of Open Area Ratio with Expansion

It is the number of slits in an expanded sheet and the area of each slit which determines the total edge area in the open area of Figure 8. If  $M$  is the width of a flat incised sheet (in a direction parallel to slit rows), then the number of slits in a row is  $M/(s + w)$  ( $s$  is slit width and  $w$  is space between slits). Similarly the number of slit rows is the length  $N$  of the unexpanded sheet in a direction perpendicular to slit rows divided by the row spacing,  $d$ , or  $N/d$ . Thus the total number of slits in a sheet before expansion is  $MN/d(s + w)$ . If the material thickness is "u", then the edge area of one slit effective in obscuring the open area in Figure 8 is  $s \cdot u$ . Therefore, the total slit edge area is

$$A_s = \frac{MN}{d} \frac{su}{s + w} \quad (3)$$

The area of the expanded sheet actually does not greatly change due to expansion, as Figure 7 suggests. Not much expansion is experienced by a sheet before significant open area is created by slit opening. Further as a sheet is expanded in length, there is some compensating contraction in width as slits pop up so that the area of a sheet after expansion may be simplified for this obscuration analysis as just  $MN$ , the flat area. Thus the edge obscuration of the open area seen in Figure 8 is

$$E = \frac{su}{d(s + w)} \quad (4)$$

where:  
 $s$  = slit length  
 $u$  = material thickness  
 $d$  = slit row spacing  
 $w$  = spacing between slits on a row

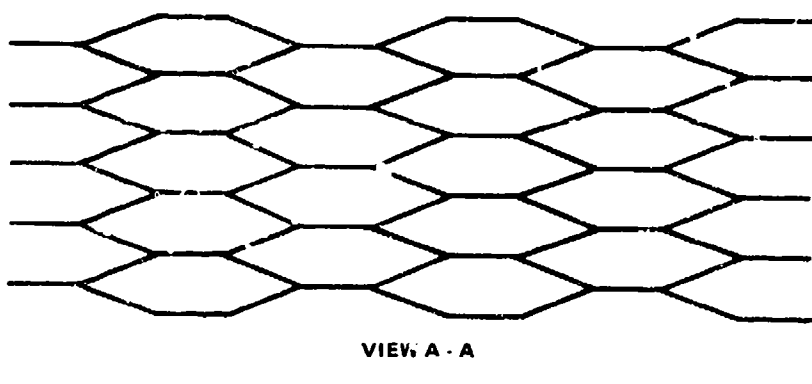


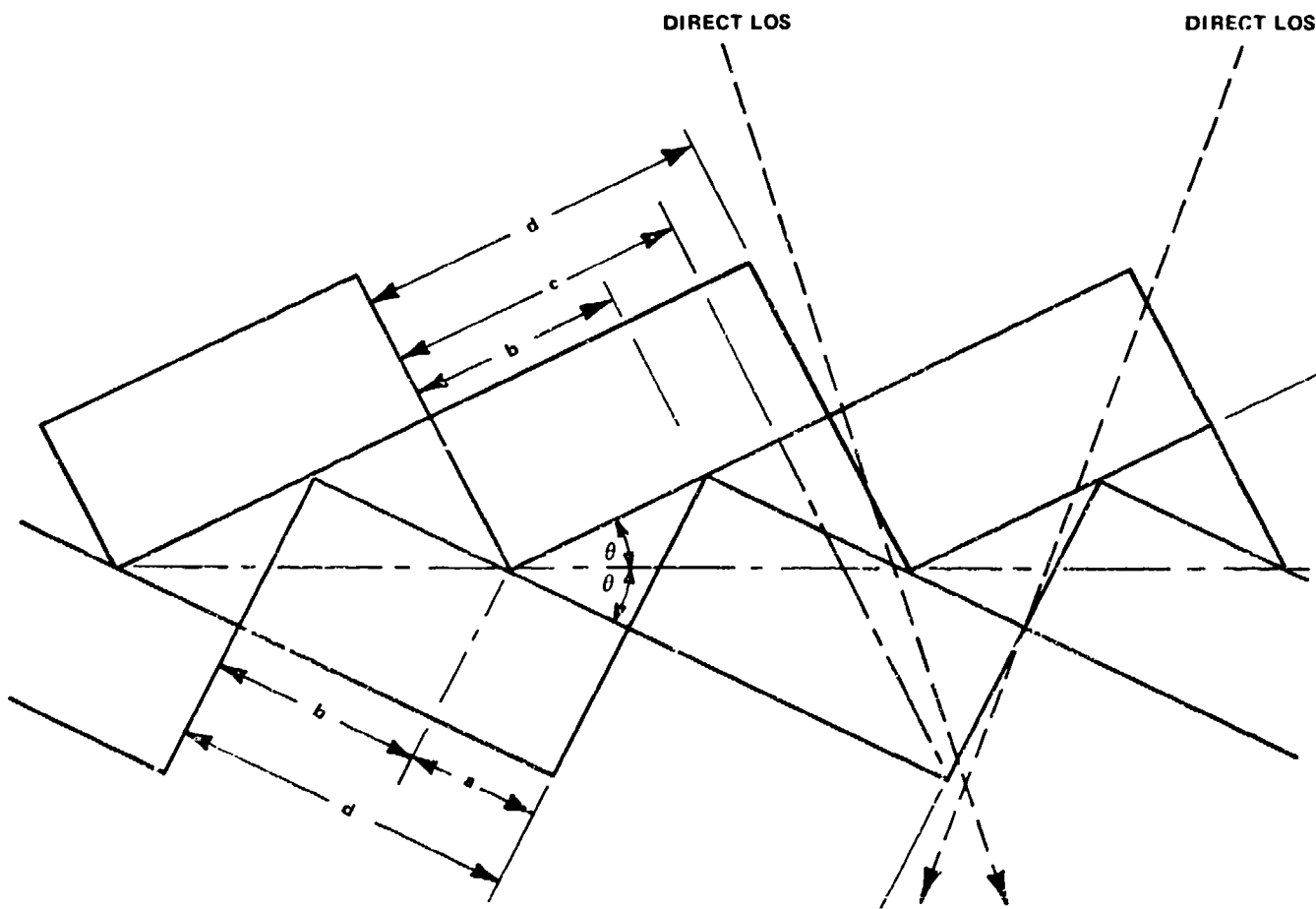
**Figure 8. Expanded Sheet Geometry - Edge View**

Some typical values for edge obscuration E are

E	Slit Length cm	Material Thickness cm	Slit Row Separation cm	Space Between Slits cm
.08	.4	.02	.2	.13
.03	1	.02	.5	.33
.02	2	.02	1	.66
.01	4	.02	2	1.33

Thus edge obscuration is not significant in many cases. Only for small slitting and relatively thick material for the slit dimensions does edge obscuration become significant. It was found in the course of experimentation with slit sheets that two expanded layers could be registered so that 100% blockage was achieved; however, for some degree of expansion 100% blockage is no longer possible. Maximum expansion is desirable for reasons of maximizing the air perfusion through the screen. Therefore, it was decided to examine the relationship of blocking and expansion angle as two sheets are placed together with openings oriented in opposite directions.

Figure 9 shows a side view of two such sheets which are each opened too far so that a direct line-of-sight (LOS) is allowed through the screen. To prevent this, the dimension labeled "c" in the figure must equal or exceed slit row spacing, d. At the angle of the sheets at which c=d, the slit openings have moved just to the point where no direct LOS is available through the pair. That defines the maximum angle  $\theta$  for the sheets and consequently the maximum expansion ratio, from equation (1).



2201

Figure 9. Geometry for Two Sheets Forming a Perfusion Screen-  
Excess Expansion Illustrated

Dimension c can be expressed as  $(a + d)\cos 2\theta$ . For maximum angle, c must equal d,

$$(a + d)\cos 2\theta_{\max} = d \quad (5)$$

Because of the symmetry of the two sheets, the ratio of a to b (subdividing d) is from the small triangle in Figure 9,

$$\frac{a}{b} = \cos 2\theta \quad (6)$$

Also trivially

$$a + b = d \quad (7)$$

The simultaneous solution of (5), (6), and (7) yields

$$a/d = (\sqrt{2} - 1)$$

$$\theta_{\max} = 22.5 \text{ degrees}$$

From equation (1) the maximum expansion ratio is then obtainable as

$$R_{\max} = 1.08$$

Thus beyond 8% expansion the two layer sheet can be expected to fail to provide 100% line-of-sight blockage. The maximum open area then can also be found to be 0.38 from (2).

This means that a two layer screen can be expanded to almost 40% open area before it starts to leak and permit an observer to look through it. Good air perfusion should,

therefore, be achievable for such a two layer screen without losing 100% blockage provided layer to layer registration is maintainable. Care in expansion will be necessary because of the sensitivity of openness to expansion (8% expansion is the limit).

#### 2.4 Tests of the Perfusion Screen.

Testing done on the perfusion screen was restricted to the assessment of thermal performance because thermal suppression was the basic thrust of this contract. Visual, near IR and radar performance were not assessed. Two modes of testing were conducted to evaluate thermal performance. Initial tests were done measuring radiometric temperatures. Later a thermal imager was also used to check radiance differences between samples and background. In both cases, the perfusion screen was tested in the form of half meter square samples mounted in stretcher frames.

Samples were prepared using spunbonded polyolefin paper about 0.010 inch thick which was slit with the straight pattern of Figure 5(a) in which slit length,  $s$ , was twice slit row separation,  $d$ , and the slit separation on a row,  $w$ , was 1/3 of slit length. That geometry was chosen because it seemed to afford good line of sight blocking and reasonable stiffness in the expanded form to retain the slit opening shapes.

Three sizes of slit sheeting were prepared with slit row separations of .5 cm, 1 cm, and 2 cm. These sheets were then spray painted with a forest green paint made according to MIL-E-52798A(ME) (type II), on both sides. This paint is intended to exhibit near IR reflectance similar to foliage.

After painting, the sheets were joined in pairs registered as the side view in Figure 9 suggests. That was to create the desired 100% line of sight blockage. The three such samples (2 layers each) were supported in stretcher frames adjusted to get the right amount of expansion.

#### 2.4.1 Radiometric temperature testing.

Radiometric temperature testing was conducted with a hand-held radiometric thermometer, making note of perfusion screen sample temperatures and background temperatures. There were two basic objectives: (1) to assess thermal response of the perfusion screen to solar load and sky cooling in comparison to the background, and (2) to note differences in that response between the three different sizes of incising (.5 cm, 1 cm, and 2 cm) which might suggest an optimum dimension. In these tests, the three samples were situated on dry brown grass (about 2-5 inches high) in a field adjacent to the Integrated Systems Division of Varo in Garland, Texas. Figure 10 shows three samples in a typical test. Near this location (within a distance of about 10 meters) were patches of tall, dry grass (about 3 feet high) and bare soil, and some hardy winter grass which was green (about 3 inches high).

Measurements which were made during these tests included:

- solar irradiance
- wind speed
- perfusion screen temperature
- air temperature
- background temperatures
- reference temperatures

Solar irradiance was measured with a simple silicon cell instrument, the Dodge Products model 776 solar meter seen on the stretcherframe of the center sample seen in Figure 10. Wind speed was measured with two instruments. One is the Datametrics VT100 hot wire anemometer most useful in low wind speed conditions down to 10 cm/sec. The other was a Taylor anemometer number 3132, a vane type instrument which averages the wind over the time chosen by the user.

One of the difficulties observed with the measurement of wind speed was that it varies widely in seconds. The response of the perfusion screen is also on the order of 5 to 40 seconds estimated from noting the change in temperature from sunlit to shaded condition. Therefore, the averaging feature of the Taylor instrument was helpful in smoothing data.

A second difficulty arose from the variability of wind direction. Both the Taylor and Datametrics instruments are sensitive to wind direction with respect to the facing direction of the instrument. To solve this problem, a wind vane was prepared on which to mount the Taylor instrument so that it would always face into the wind as desired. Figure 11 is a photograph of the Taylor anemometer mounted on this wind vane.

The key instrument for making radiometric temperature measurements was the Raytek model R2LT non-contact thermometer. It senses radiant power in the 8 to 12 micron waveband and converts this power into a temperature, based on the emissivity setting of the instrument. All test measurements were made with the emissivity setting at 1.00 so that equivalent blackbody radiometric temperatures would be read. Appendix A discusses a correction made when using

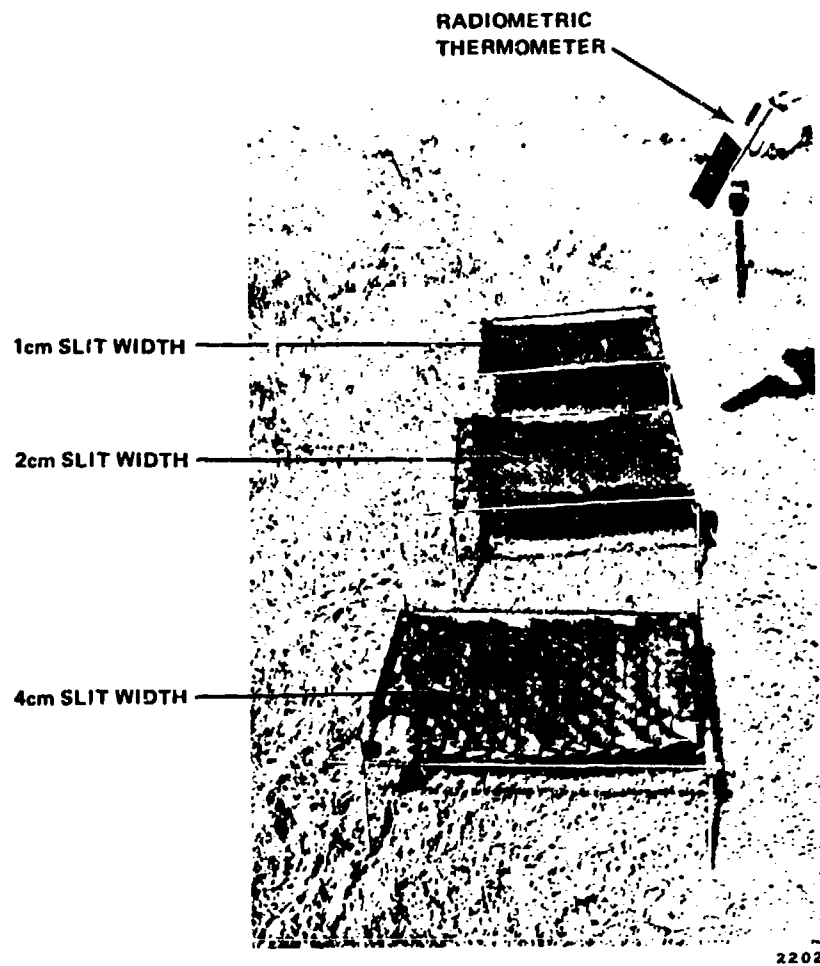
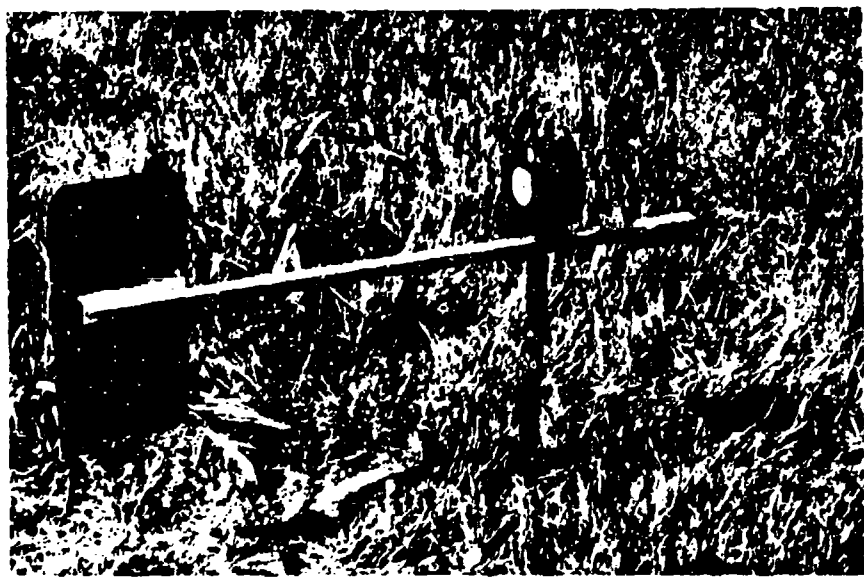


**Figure 10. Samples for Radiometric Temperature Testing at the Test Site**



2203

**Figure 11. Wind Vane for Wind Speed Measurement**

the R2LT for measuring screen temperature to take into account the fact that the instrument makes no discrimination of power emitted by the surface at which it is aimed from power reflected by that surface. The procedure in Appendix A permits getting actual temperature data for model calculations from radiometric temperatures. Sensing the combined effect of emitted and reflected power is precisely what thermal imagers do as well. Therefore, the R2LT gives a measure of the total power emanating from objects at which it is aimed in the form of radiometric temperatures. This permits an assessment of perfusion screen radiant difference with background as desired in a realistic way.

The R2LT was also used to make a radiometric assessment of air temperature by pointing it at specially prepared vanes forced to air temperature by drawing air through them rapidly. This radiometric reference temperature measurement is presented in Appendix B.

Another reference temperature needed for the thermal model of the perfusion screen is effective sky temperature. What was actually measured was the radiometric temperature of a white insulation pad laid on the ground and shaded. This temperature along with other measured parameters permitted a calculation of effective sky blackbody temperature. That procedure is presented in Appendix C.

#### 2.4.1.1 Results of radiometric temperature testing.

Figures 12 and 13 summarize field test measurements of radiometric blackbody temperature for the perfusion canopy samples and items in the background. Heavy bars correspond to radiometric temperatures for camouflage samples and lighter bars are for background items.

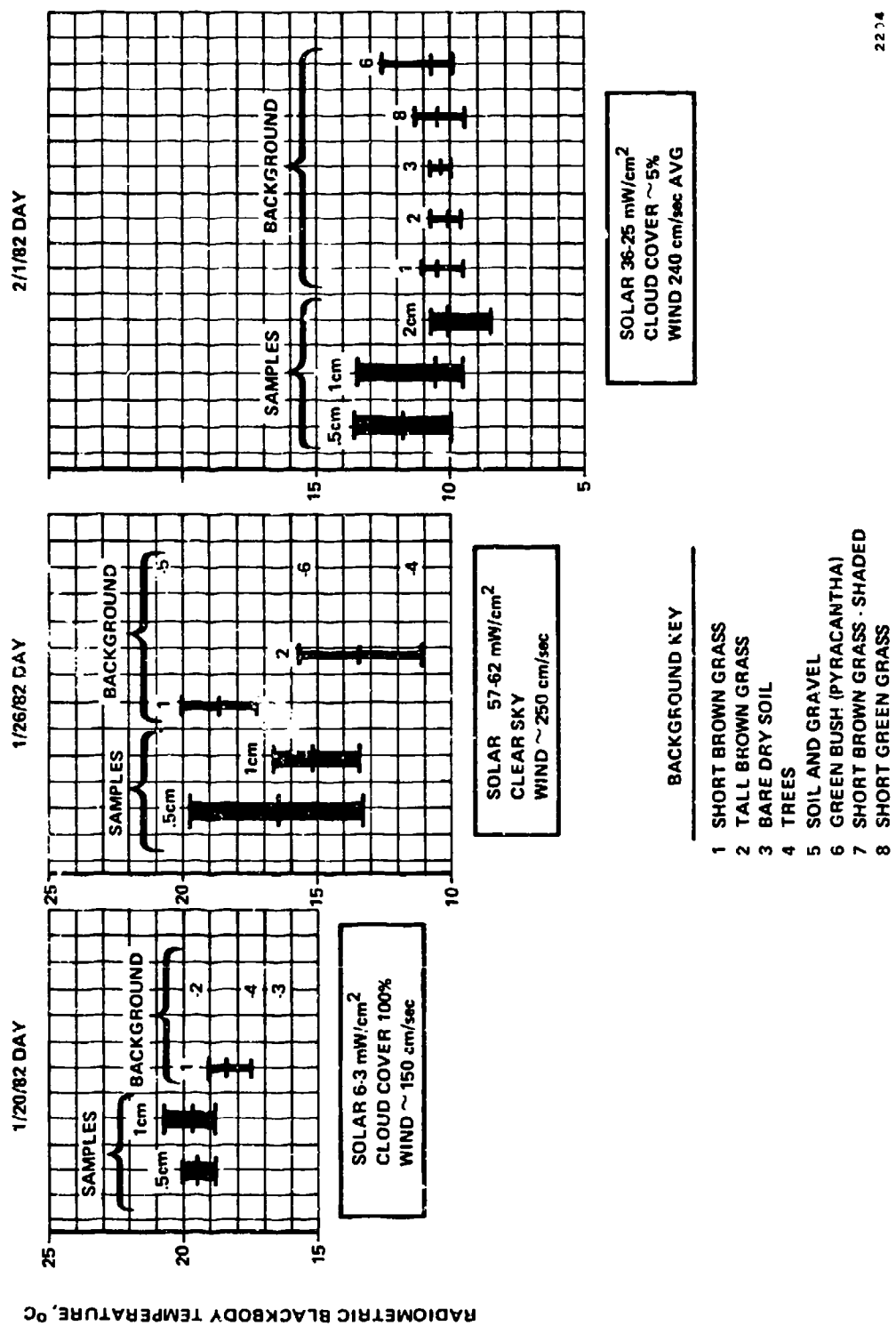


Figure 12. Radiometric Temperatures of Perfusion Screen Samples and Background on 1/20/82, 1/26/82, and 2/1/82 in the Day

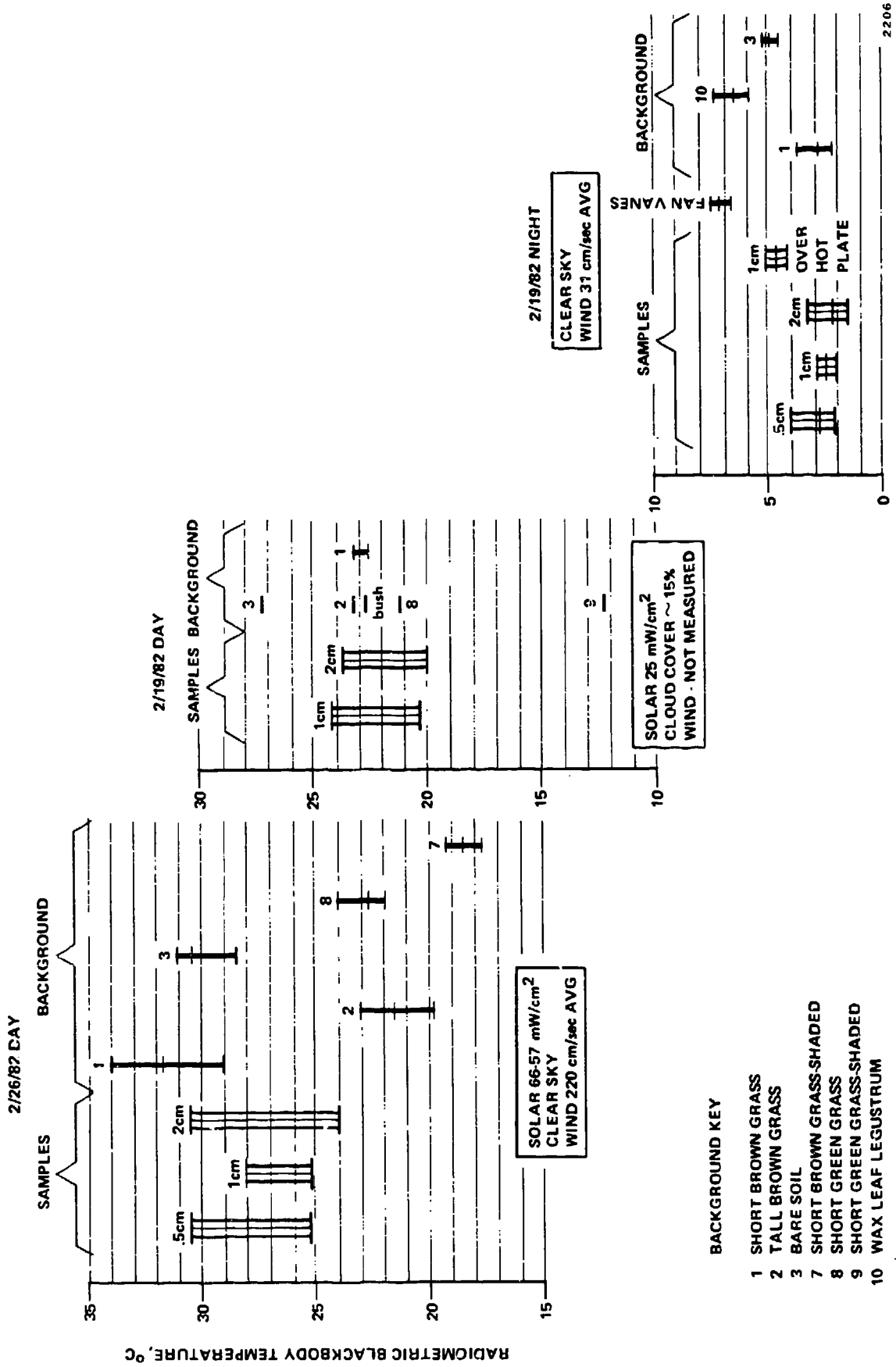


Figure 13. Radiometric Temperatures of Perfusion Screen Samples and Background on 2/16/82 and 2/19/82 in the Day and 2/19/82 at Night

End points of the bars are max and min values. The intermediate line on each bar is the average radiometric temperature for that bar. In some cases there was only one measurement and that is shown as a single line.

Tests in January were done with only two samples of the perfusion screen. Later, to more fully explore the effect of dimension, another sample was added with 2 cm slit row separation. That was done because the earlier tests did not show expected differentiation between .5 and 1 cm row separation screens.

The January 20, 1982 test shows that the two screens tested were about a degree Celcius warmer than short brown grass and about the same as the single measurement of tall brown grass. On January 26, 1982, the results were that the samples were thermally situated between short brown grass and tall brown grass. This was in a clear sky condition whereas the 1/20 test was under a fully overcast sky. On February 1, 1982, when three samples were used, the 1 cm and 2 cm samples were just about an exact match with grass (1, 2, 8) and bare soil (3). This was again a clear day although the solar load was low.

On the 2/16 test all samples averaged within half a degree C of each other and fell nicely in between the background measurements. The 2/19 test shows test samples also within background. Note again the condition was low solar and low cloud cover.

A night test was run on 2/19. Figure 13 shows that perfusion screen temperatures were very close to those for dry brown grass. They were a little cooler than bare soil or leafy vegetation.

On this night also the first experimentation with a hot plate in an outdoor test was conducted. The 1 cm sample was placed over a 6 inch square hot plate with a separation of about 6 inches between the hot plate and the test screen. The hot plate was 24°C warmer than air. The test screen temperature rose about 2°C due to this heat source in slowly moving air (velocity 50 cm/sec) coming to a temperature nearly the same as bare soil with temperatures between a legustrum bush (green leaves) and short brown grass.

Radiometric air temperature measurement with the fan vanes, also shown on the figure for the night test, shows that the perfusion screen samples were about 4 to 5 degrees C cooler than air. (See Appendix B for a discussion of the fan vanes).

#### 2.4.1.2 Conclusions from radiometric temperature tests.

This set of results indicates good performance for the screens. Average screen temperatures were within the background variation for the conditions under which tests were made. There seems to be a trend that clear sky conditions cause the perfusion screens to fit into the background temperature variation better. Despite the very low solar load ( $6\text{mW/cm}^2$  or less) the overcast condition on 1/20/82 (Figure 12) shows a tendency for the screens to rise to the top end of the background variation. However, background data were sparse for that test; so all that can be said is it suggests the possibility of overcast condition upward influence on screen temperature.

One of the objectives of using three samples of perfusion screen was to evaluate the effect of slit dimension. It was anticipated that the smallest size of

slit (all were proportionally cut) would produce the greatest convective coupling to air temperature. There is a slight indication from these tests that the smallest slit dimension (0.5 cm row spacing) was warmer than other samples. That would show less convective coupling overall.

The details of analyzing what was taking place thermally will be addressed in section 2.5.3.3. There a "perfusion factor" is introduced which attempts to allow for a change in the degree of openness to air flow through the screen (perfusion) with significant length.

Nevertheless, it may be concluded that the anticipated variation of screen temperature with dimension is not supported by these tests.

These data would suggest that perhaps the 2 cm slit dimension performed slightly better than the other two. In addition the 2 cm perfusion screen is easier to make.

#### 2.4.2 Imaging tests.

Following the initial test series done only with the radiometric temperature instrument, a commercial thermal imager was rented for imaging testing. The instrument used was the Inframetrics model 525 thermal imager operating in the 8-12 micrometer range. Detailed specifications on the imager are given in Appendix E. The system is, however, compatible with video recording which was the method of documentation used.

Actual imaging of the screens provided data more closely related to what would be experienced in an actual thermal camouflage situation. It in effect provides many radiant measurements very quickly so that temporal and areal effects can be observed. Among temporal effects which can be seen are radiance shifts due to intermittent sun (clouds passing over) and wind speed changes. Areal effects such as mottling and on a larger scale, differences in the ambient (from grass to bush to bare soil) are simultaneously available because of the 30 hz frame rate. One of the matters which it was thought the image tests could determine was what differences there are in performance of the three different dimensions of perfusion screen. When separate measurements must be made as with the radiometric thermometer, the change in wind and sun between readings obscures effects due to screen dimension. The imager thus offered a better tool with which to examine the screen differences thermally at the same time for the prevailing ambient conditions.

#### 2.4.2.1 Imaging tests description.

Imaging tests were conducted at the same general location as the temperature tests - on a grassy area north of the Integrated Systems Division of Varo in Garland, Texas. The same samples were used (slit lengths of 1, 2, and 4 cm).

As an aid to evaluating background temperatures, a section of grass adjacent to the position of the perfusion screens was removed to leave bare soil about one day prior to the first test. That area was roughly the same size as one test screen. The imager was positioned some 10 meters from the row of perfusion screens and the associated environmental equipment set up nearby.

While imagery was taken solar load and wind (average for 15 seconds normally) were also measured. In addition, a set of temperature measurements on the screens and background were made in the same way as radiometric temperature testing.

While imagery was being video tape recorded, audio dubbing was put on to explain what was happening.

Various other materials were also used for comparison with the screen samples. In particular, the former thermal blanket was used. It consisted of three each 1/4 inch thick polyolefin foam insulating layers inside an olive drab ripstop cover (polyurethane olive drab coloring on the ripstop). It was of interest because of its former application to thermal camouflage and the attendant problems it experienced in solar overheating and nighttime overcooling. Since the visual net is widely used, it was thought desirable to test, along with the perfusion screens on occasion, a section of visual screen next to the screen samples.

#### 2.4.2.2 Imaging Test Results

Results of imaging tests are shown in photos from the video monitor of recorded imagery.

Figures 14-17 are images from the night test on 3/18/82. Figures 14 and 15 show the appearance of the three test screens and some background items. Two containers were placed behind the samples with branches from a pyracantha bush and a cedar tree in them. They are visible in Figure 15. The patch of bare soil is just left of screen 1 (slit width of 1cm) in Figure 14. The screens appear to have radiance levels about the same as the two foliage branches which is regarded as a good result. No overcooling due to the influence of cold sky was seen for the perfusion screens.

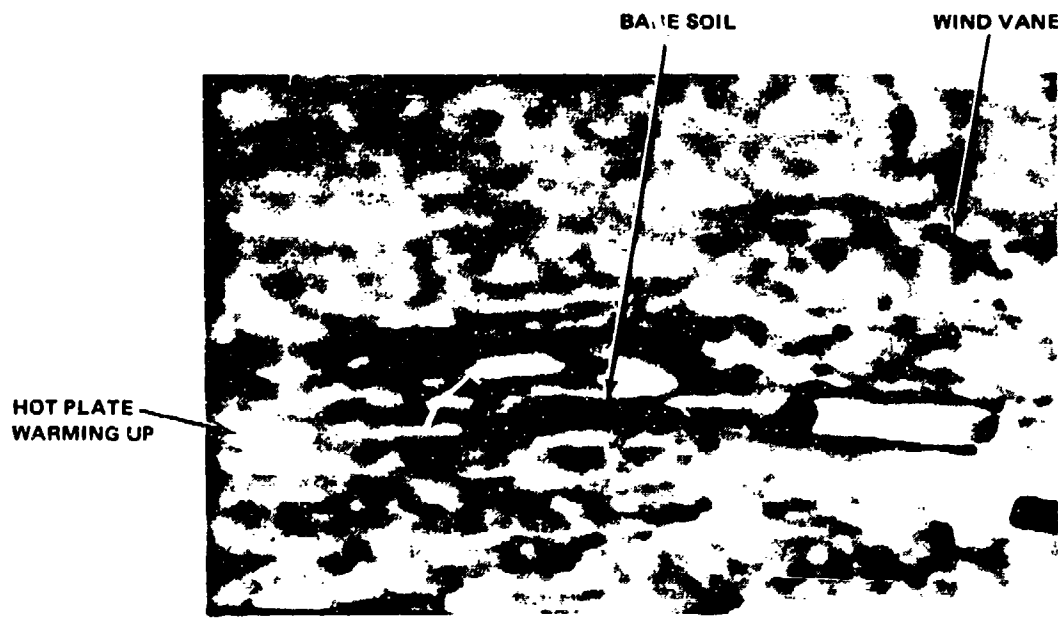


Figure 14. Night Imagery - 19.55 on 3/18/82

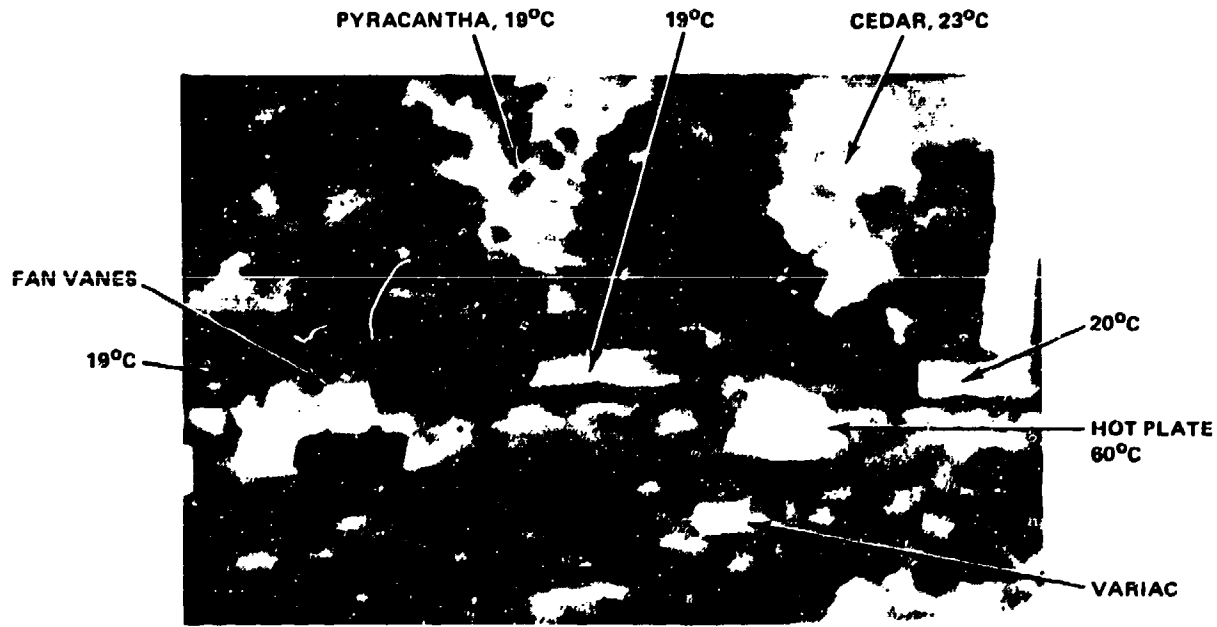


Figure 15. Night Imagery - 20:21 on 3/18/82

2205

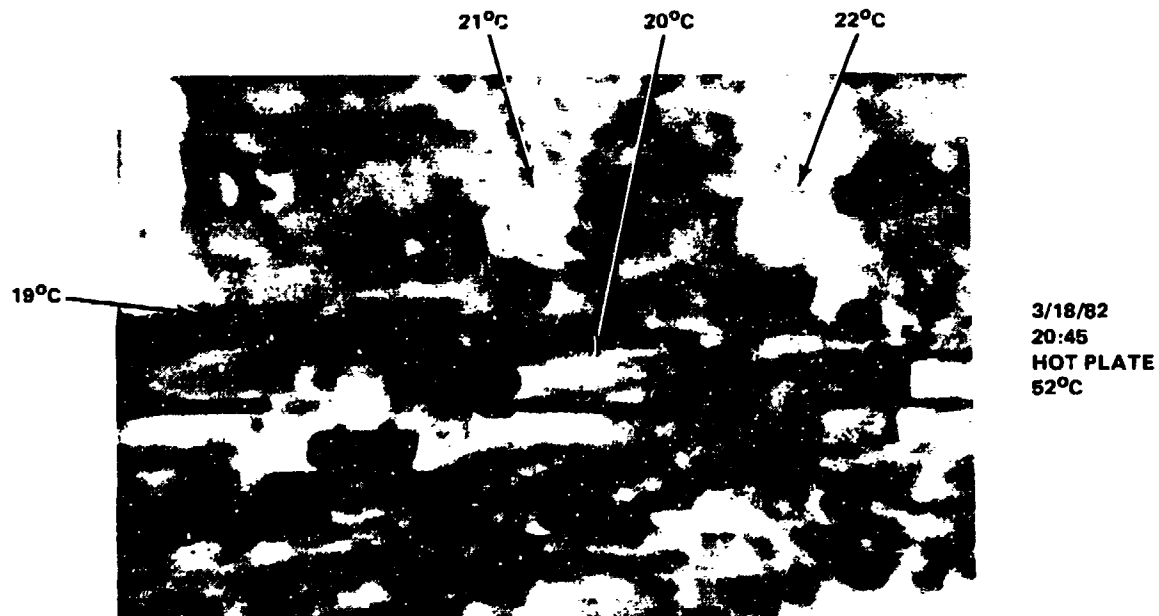


Figure 16. Night Imagery - 20:45 on 3/18/82 with Screen 2  
Over a Hot Plate

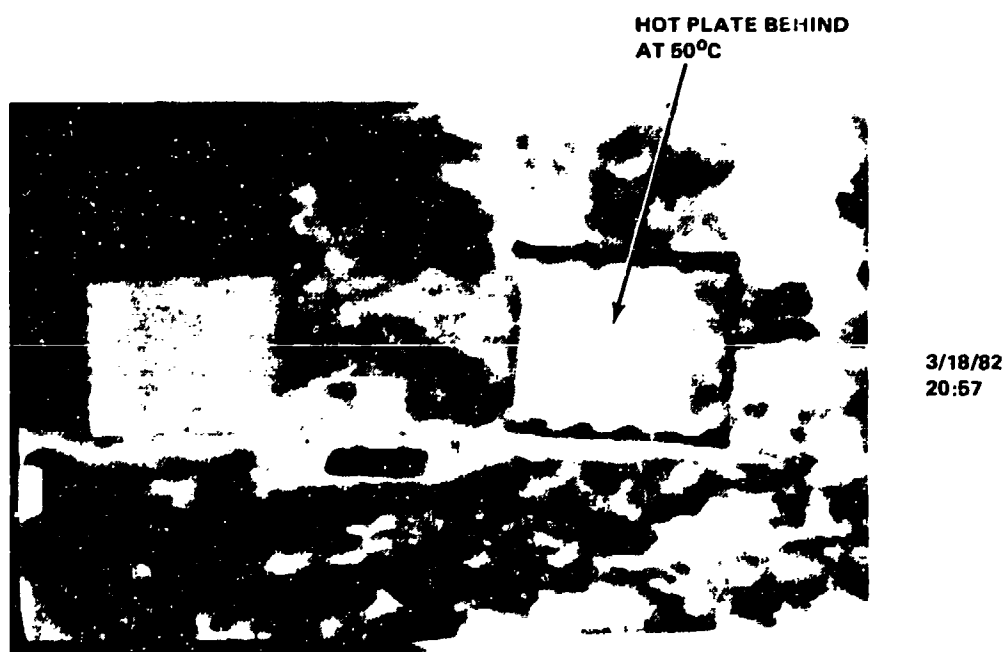


Figure 17. Night Imagery with 2cm Slit Width Perfusion  
Screen Vertical in Front of Hot Plate

2207

The white object in 14 is a 6 inch square hot plate which was placed under screen 2 about 6 minutes before the video taping of imagery in Figure 16 was made. This was done to experiment with the effect of convective heating which might present a problem to the screen, since it is designed to be penetrated by air flow and to assure blocking of direct view thermally. The figure shows no damaging effect in this case. Air gap between the screen and the hot plate was about 4 inches.

Because the influence of cooling to the sky was expected to be strong, there was some curiosity about the effect of diminishing sky cooling by placing the screens in a vertical orientation. This was done for screen samples 1 and 2 which are seen in Figure 17 with the fan vanes in between.

In addition, the hot plate was moved to a vertical position about 4 inches behind the center of screen number 2 (on the right side in the figure). Radiometric blackbody temperature of the hot plate was 50°C. - about 28°C warmer than air temperature. The wind was blowing generally from the camera site towards the samples so that it would tend to carry heat from the hot plate away from the screen. Only a very slight effect is observable due to the presence of the hot plate.

Radiometric blackbody temperatures which were measured during the course of the night imaging are presented in Figure 18 in the form of bar graphs. As in similar bar graphs for the temperature tests, the total excursion is given for each item and the average temperature shown as a horizontal line in each bar.

There was little difference among the screen samples and particularly none was too cold (colder than the

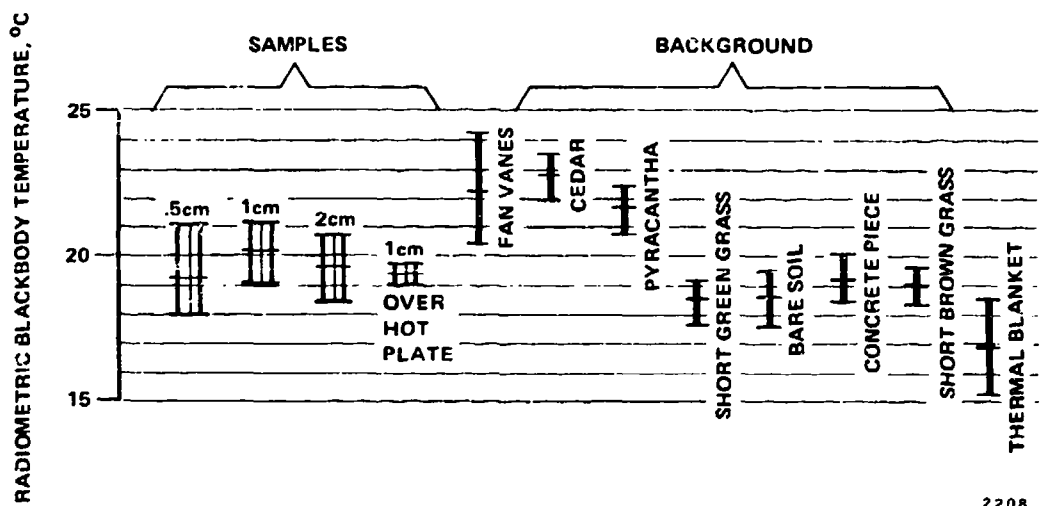


Figure 18. Radiometric Blackbody Temperatures of Perfusion Screen Samples and Background on 3/18/82 at Night

background). They were close to the temperature of short brown grass. Though not in the imagery, the thermal blanket was colder than the background by a small amount.

In Figures 19 and 20 are results of imaging in a high solar load and high cloud cover condition. That results in screen temperatures elevated over that of background grass, but closer to that of bare soil which also responded to the solar heating. Bare soil shows in Figure 19 at the left side. This condition is probably a worst case for heating of the screens because it minimizes sky cooling due to the presence of clouds which are much warmer than a clear sky while rifts in clouds can still permit high solar load to fall on the screens. In this condition, therefore, the screens do tend to warm up though not nearly to the extent that the thermal blanket does. In Figure 20, the thermal blanket radiometric blackbody temperature was measured at about 52°C - some 18°C hotter than the screens.

Figures 21-23 are a set demonstrating the improvement in screen performance in high cloud cover when the solar load goes from high to low. Figure 21 shows the visual appearance of the samples and foliage in containers just behind them. Figure 22 shows the two screens (1 and 2cm slit width) in a solar load of about  $60 \text{ mW/cm}^2$  and about 80% cloud cover. When the solar load fell to about  $30 \text{ mW/cm}^2$  (due to a cloud blocking the sun) temperatures of the screens fell to levels closer to that of grass and lower than bare soil (white patch left of screen sample 1 in Figure 23).

Bar graphs of radiometric blackbody temperatures measured during 3/17/82 daytime testing are given in Figure 24. The length of the screen bars shows the variation with fluctuating solar load as clouds blocked the sun. Average temperatures of the samples are shown there to be close to bare soil and the concrete piece. Green vegetation (cedar, pyracantha, and green grass) all had temperatures close to that of the fan vanes. That, in turn, is a representation of

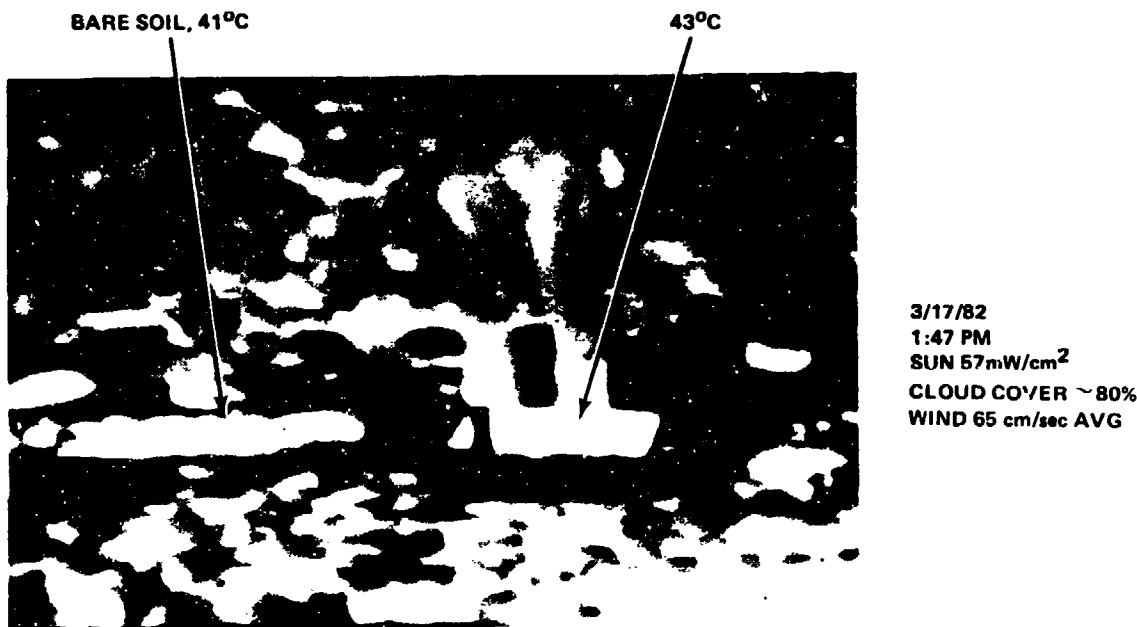


Figure 19. Day Imagery - High Solar, High Cloud Cover.  
Screen 1 and Bare Soil

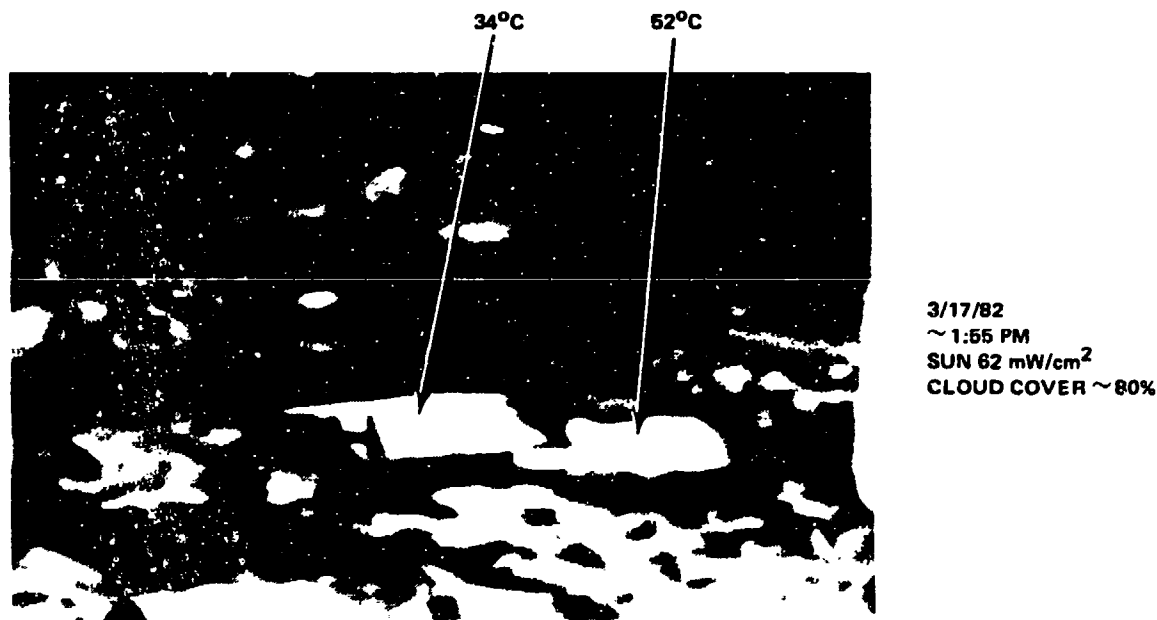


Figure 20. Day Imagery - High Solar, High Cloud Cover.  
Screen 4 and Blanket

2209

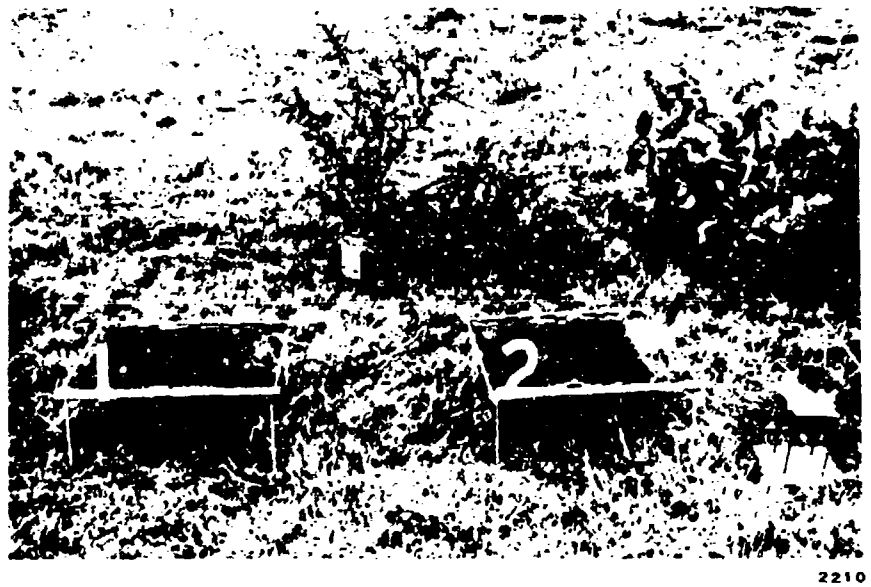


Figure 21. Visual Photograph of Test Items on 3/17/82



3/17/82  
~ 1:50 PM  
SUN ~ 59 mW/cm<sup>2</sup>  
CLOUD COVER ~ 80%

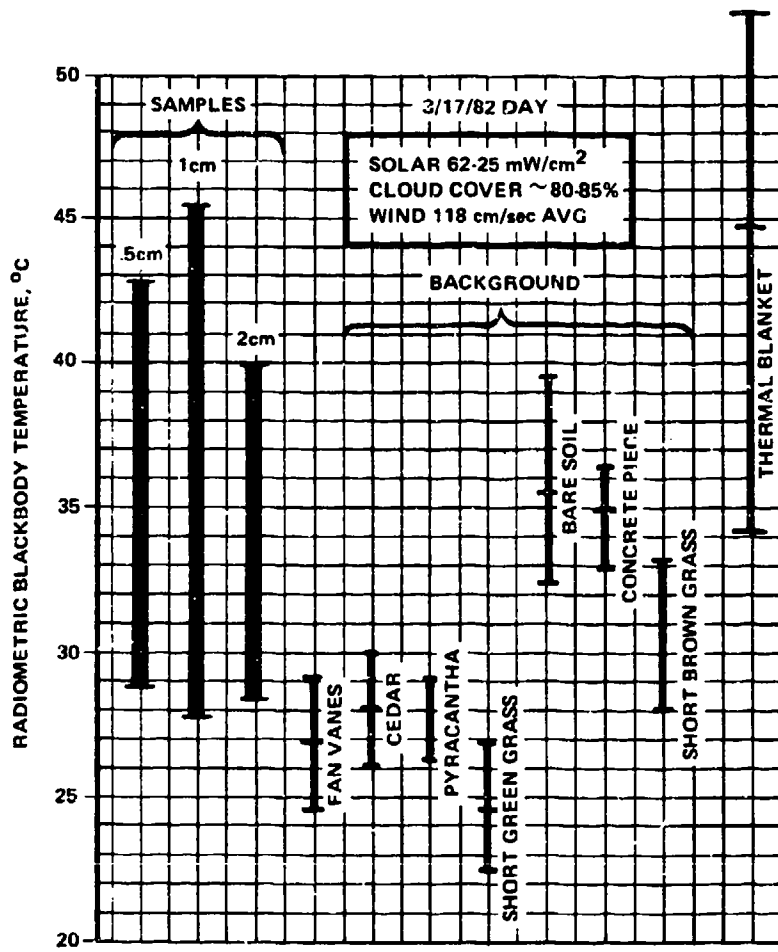
Figure 22. Day Imagery - High Solar, High Cloud Cover  
Screens 1 and 2



3/17/82  
~ 2:10 PM  
SUN ~ 30 mW/cm<sup>2</sup>  
CLOUD COVER ~ 85%

2211

Figure 23. Day Imagery - Low Solar, High Cloud Cover  
Bare Soil, Screens 1 and 2



2212

Figure 24. Radiometric Blackbody Temperatures of Perfusion Screen Samples and Background on 3/17/82 in the Afternoon

radiometric air temperature since the fan vanes were forced to air temperature by the electric fan drawing air through them. The relative coolness of the green vegetation is attributed to transpiration.

Again, the thermal blanket is clearly outside the temperature range of the background objects which were measured in this test.

Figures 25-27 correspond to low cloud cover conditions. The visual photograph in Figure 25 is to show the relative positions of samples and background foliage. Note as well that there is a section of visual camouflage screen (spring and summer side up) placed between samples 1 and 2 with the fan vanes in front of it.

Figure 26 shows some morning imagery in which the screen samples 1, 2 and 4 were warmer than the average background. There were some areas of background, however, which show as warm as the perfusion screens or warmer. The contrast or level control should actually have been set lower to get better dynamic range and allow the warmer background objects to show without saturation. Apparently the saturation level was high enough in the case of the thermal blanket that there was some blooming around it. Thus it was the warmest object in the field-of-view. In this instance, the visual screen was cool.

Now, in the early afternoon on 4/5/82, when solar load was the highest measured during testing, but there was insignificant cloud cover, the perfusion screen samples in Figure 27 are satisfactorily within background variation in the picture. This was green and brown grass.

Thus with the help of radiation cooling to the clear sky, the perfusion screen samples appear to be able to cope with a high solar load satisfactorily. The visual screen in this condition also appears about the same as the perfusion



Figure 25. Visual Photograph for 4/5/82 Testing

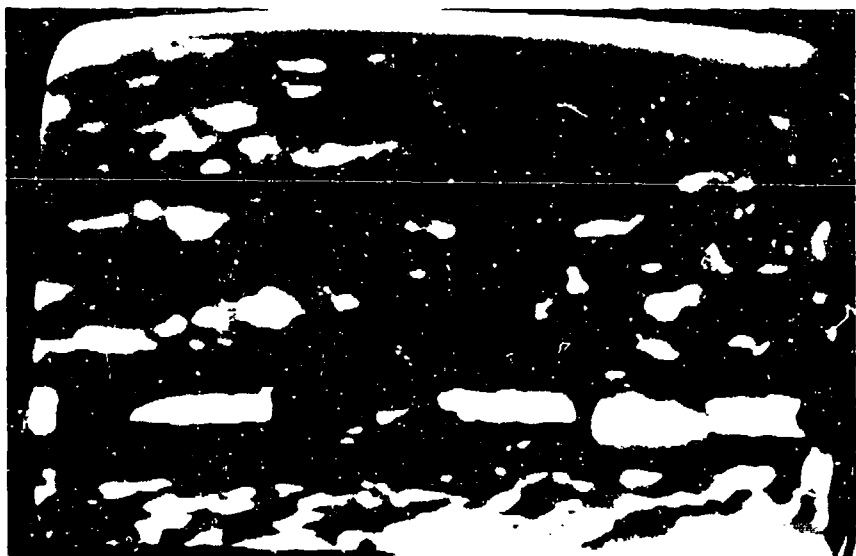
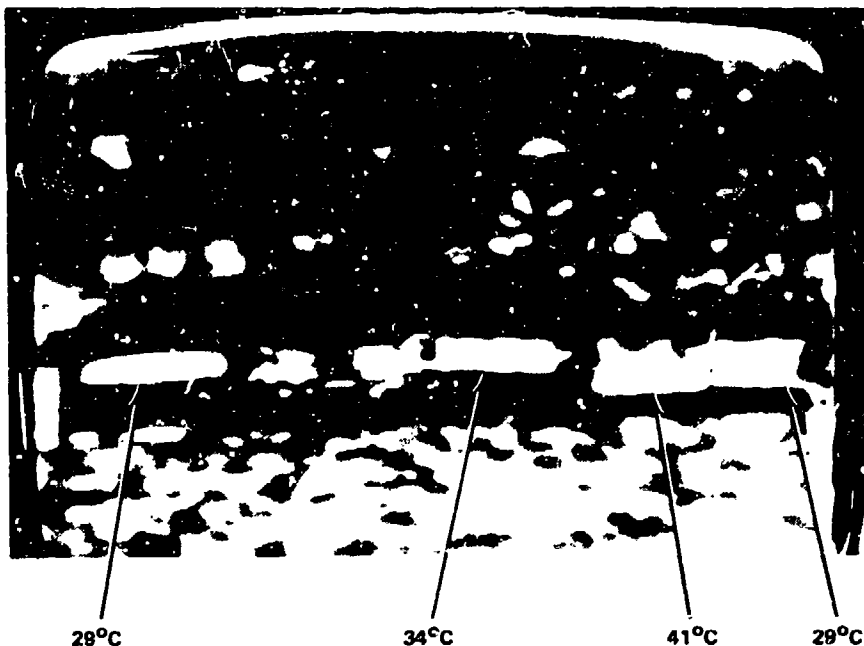


Figure 26. Morning Imagery - Low Cloud Cover

2213



4/5/62  
~ 1:51 PM  
SUN 85 mW/cm<sup>2</sup>  
CLOUD COVER ~5%  
WIND 245 cm/sec AVG

2214

Figure 27. Day Imagery - High Solar, Low Cloud Cover

screen. Once again the thermal blanket was excessively warm.

Figure 28 is another bar graph of the clear sky condition testing. It verifies the performance noted from imagery. The perfusion screens were at about the temperature of short, brown grass as was the visual screen. Green vegetation was at the lower range of background variation and the thermal blanket riding above everything.

Figures 29 and 30 are imagery taken of a vertical perfusion screen with a hot plate behind it. In the second of these two figures (Figure 30), a surface garnishment has been added. Garnishing was paper material which was incised with about a 1.8mm slit row separation expanded and then re-incised with the visual incising pattern (interlocking curves), forming a lacy garnishment. Figure 31 is a photograph of the screen with this garnishment on it.

#### 2.4.2.3 Imaging Tests Conclusions

The tests demonstrated that there is a marked improvement in thermal performance for the perfusion screen samples as compared to the thermal blanket which did overheat in solar load. The screens were definitely cooler. However, in some environmental conditions, the perfusion screens tended to rise in radiometric blackbody temperature toward the upper end of background objects (bare soil, concrete piece). That may not be suitable in some instances (in which bare soil or rocky areas are absent and those conditions exist). The severe condition is a high solar load and at the same time high cloud cover. Interestingly though, even in high solar load condition if the sky is clear, perfusion screens appeared to cope with the solar heat adequately (radiometric temperatures within the background variation).

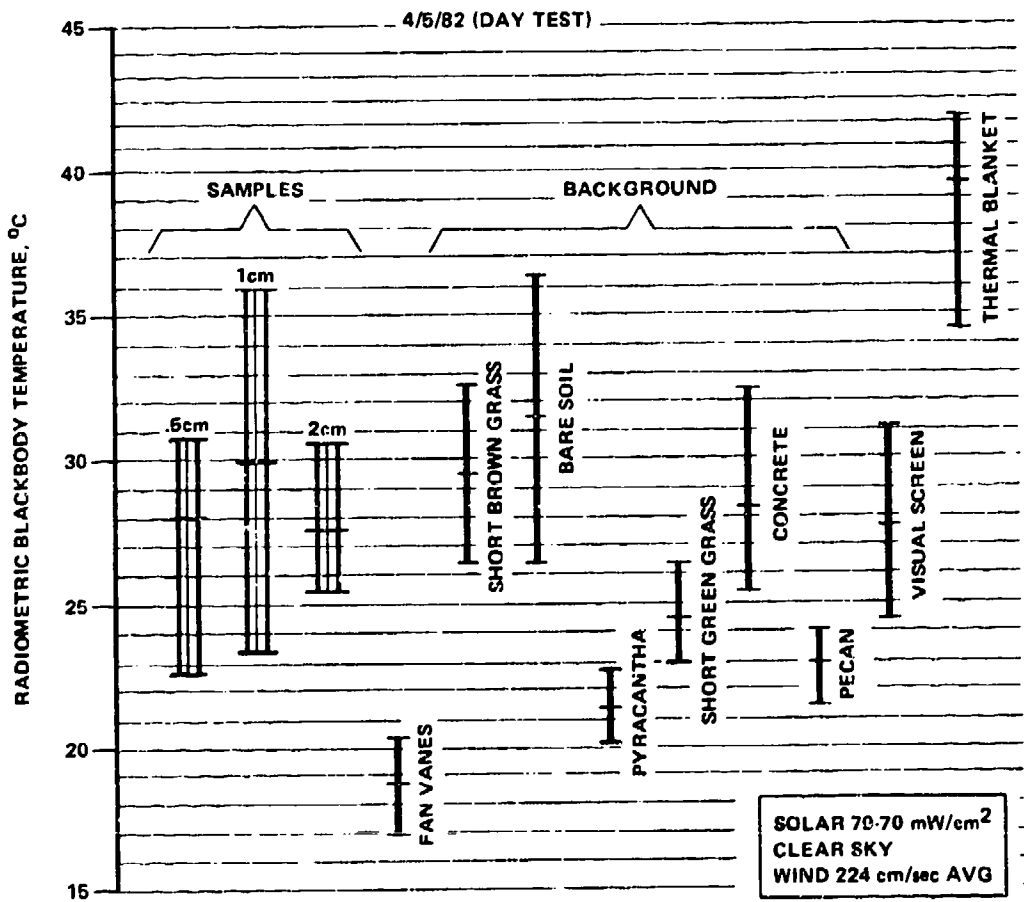


Figure 28. Radiometric Blackbody Temperatures of Perfusion Screen Samples and Background on 4/5/82 in the Day



4/5/82  
2:45  
HOT PLATE 5 IN  
BEHIND

Figure 29. Day Imagery - Vertical Perfusion Screen



4/5/82  
2:55 PM  
SUN 70mW/cm<sup>2</sup>

221G

Figure 30. Day Imagery - Garnishment on Vertical Perfusion Screen

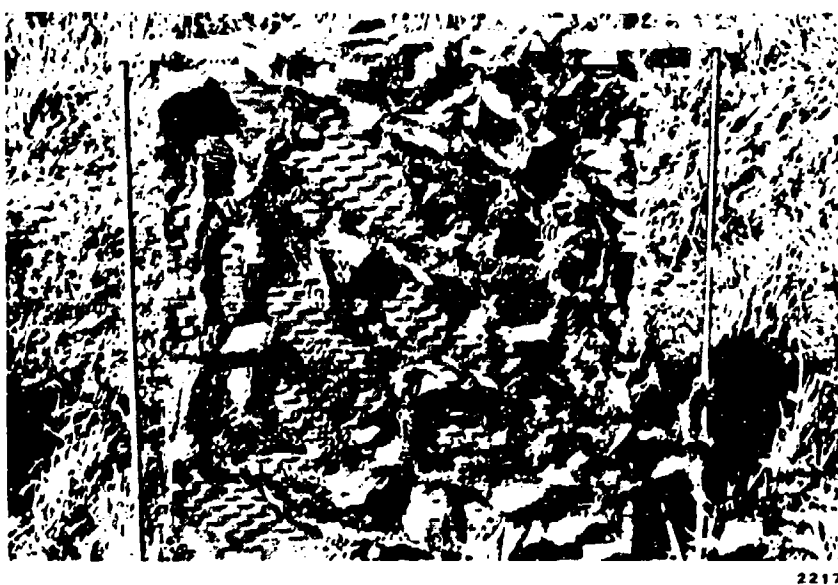


**Figure 31. Vertical Perfusion Screen with Double-incised Garnishment Added - Two Layers**

When high cloud cover exists and the sun is blocked, the initial results suggest that there will be no particular problem for the screens in overheating.

The single night test on 3/18/82 did not indicate any problem with overcooling at all. The screens all performed well. They appeared to blend reasonably with the test background.

Orientation of the perfusion screens was looked at briefly by placing screens vertically on several tests. No striking effects or differences were noted from the predominantly horizontal placement of screens because of moving them to the vertical.

Experimentation with a hot plate under or behind a screen showed no direct infrared transmission indicating the materials were absorbing and that there were no holes for direct line-of-sight to the hot plate from the thermal camera. Such direct view was, of course, observed with the visual screen placed in front of the hot plate. In addition, perfusion screen heating due to proximity of the hot plate was not noticeable when the spacing from hot plate to screen was 6 inches. Even at 4 inch separation, the effect was just discernable (see figure 16). This suggests that the perfusion screen may not have to be emplaced at large separations from targets which it is designed to conceal.

The experimentation with surface garnishment did show potential for generation of thermal mottling in this way. Further, there was some indication that such garnishment could alleviate to some extent, heating due to solar load if that were deemed necessary.

Finally, one matter which was addressable with imaging tests, was differentiation between different perfusion screen dimensions to note optimum. The imaging tests did

not show thermal differences between the 1, 2 and 4cm slit width screens which were regarded as significant. Therefore, unless later testing does point up a difference, the present indication is that other factors than thermal performance can be used to make selection of slit dimension. Since the 2cm slit width screen is easier to make, it may be the choice.

## 2.5 Thermal Equations for the Perfusion Screen

### 2.5.1 Heat Balance Equation

The temperature of thermal camouflage is stabilized when the net heat input is equal to the net heat output. The potential sources of heat input are solar irradiance, thermal radiation from the sky, and thermal radiation from the ground. The heat output results from thermal radiation to the sky, thermal radiation to the ground, and forced convection heat exchange with the air. Free convection is not considered in the model because outdoor conditions are expected to produce forced convection almost exclusively.

Solar heat input depends on the absorptance at the camouflage surface. We assume that solar energy is not transmitted through the camouflage material and that the radiation which is not absorbed is reflected. In addition, the camouflage long wave (thermal) transmittance is assumed to be zero. Under this assumption, the thermal radiation from the sky and ground which is not absorbed by the camouflage, is reflected. It combines with the emitted energy leaving the canopy.

The model also assumes that solar and thermal energy leaving the camouflage is not reflected back to the camouflage.

With the above assumptions, the heat balance equation is

$$\alpha H + \alpha_t q_{fs} + \alpha_t q_{fg} = q_{ts} + q_{tg} + q_{c,a} \quad (8)$$

where  $\alpha$  = solar absorptance

$\alpha_t$  = thermal absorptance ( $> 2 \mu\text{m}$ )

$H$  = solar irradiance

$q_{fs}$  = thermal radiation from sky

$q_{fg}$  = thermal radiation from ground

$q_{ts}$  = thermal radiation toward sky

$q_{tg}$  = thermal radiation toward ground

$q_{c,a}$  = convection heat loss from camouflage

### 2.5.2 Radiation Terms

Radiation terms in equation (8) can be written as the product of Stefan-Boltzmann constant,  $\sigma$ , and the fourth power of blackbody temperature,

$$q_{fs} = \sigma T_{sbb}^4 \quad (9)$$

$$q_{ts} = q_{tg} = \sigma T_{cbb}^4 \quad (10)$$

$$q_{fg} = \sigma T'_{gbb}^4 \quad (11)$$

where:

$T_{sbb}$  = sky blackbody temperature

$T_{cbb}$  = camouflage blackbody temperature

$T'_{gbb}$  = radiometric blackbody temperature of the ground

The last term,  $q_{fg}$ , is assumed to include power reflected from the ground as well as that emitted by the ground. For that reason the prime is inserted on the temperature. It is convenient to note that a radiometric blackbody temperature

measurement of the ground yields just this temperature. A radiometric thermometer simply computes an equivalent target temperature which would have produced the effect of the combined emitted and reflected power at the instrument. In subsequent discussion, the term "radiometric blackbody temperature" will be used to mean such temperatures measured with a radiometric thermometer with emissivity set to one. These temperatures will be higher than blackbody temperature (corresponding to emitted power only) by an amount depending on the strength of reflected radiation. Appendix A addresses this point.

### 2.5.3 Convection Term

The procedure for developing the convection term in the following will be first to present the idealized convection equation. This expression is then modified, by introducing an empirical parameter to account for heat transfer by forced convection through the incised openings in the perfusion canopy.

#### 2.5.3.1 Idealized Convection Equations

The convection heat transfer term is

$$q_{c,a} = 2h (T_{cam} - T_{air}) \quad (12)$$

where:

$T_{air}$  = actual air temperature

$h$  = heat transfer coefficient

The factor of two arises because there is convection on both the top and bottom sides of the perfusion screen slit elements. In terms of free stream air velocity,  $V$ , and the significant length,  $L$ , over which convection occurs,  $h$  is given by

$$h = K_c \sqrt{\frac{V}{L}} \quad (13)$$

In Equation 13,  $K_c$  is defined to be the "forced convection factor".  $K_c$  is evaluated using the theoretical model for parallel air flow over a flat plate at constant temperature (Ref 1). This approach is taken in order to separate out the free stream air velocity, and the significant length, which depends on the physical size and geometrical shape of the incised pattern in the perfusion canopy. The idealized convection equation is therefore

$$q_{c,a} = 2 K_c \sqrt{\frac{V}{L}} (T_{cam} - T_{air}) \quad (14)$$

In order to determine  $K_c$ , we use the theoretical result from Ref. 1, equation 7, for forced convection from a plate having a uniform surface temperature.

$$\text{Nu} \text{Re}^{-\frac{1}{4}} = 0.6 \quad (15)$$

where  $\text{Nu}$  is the Nusselt number and  $\text{Re}$  is the Reynolds number.  $\text{Nu}$  and  $\text{Re}$  are non-dimensional quantities defined as

$$\text{Nu} = hL/\kappa$$

$$\text{Re} = VL\rho/\mu$$

where  $\kappa$  = thermal conductivity of air

$\rho$  = density of air

$\mu$  = dynamic viscosity of air

Substitution into Equation 15 and solving for  $h$  gives

$$h = 0.6 k \sqrt{\frac{\rho}{\mu}} \cdot \sqrt{\frac{V}{L}} \quad (16)$$

Comparing Equation 16 with Equation 13, we have

$$K_c = 0.6 k \sqrt{\frac{\rho}{\mu}} \quad (17)$$

Measured values for the parameters  $k$ ,  $\rho$  and  $\mu$  are in Table A-5 of Reference 2. At a temperature of 300K

$$k = 0.02624 \text{ W/m}\cdot\text{K}$$

$$\rho = 1.1774 \text{ kg/m}^3$$

$$\mu = 1.983 \times 10^{-5} \text{ kg/m}\cdot\text{sec}$$

Substitution into Equation 17 gives

$$K_c = 0.39 \text{ mW}\sqrt{\text{sec}} / \text{cm}^2\text{K}$$

At a temperature of 350K,  $K_c$  increases by only 2%. It is assumed, therefore, that  $K_c$  is independent of temperature for the temperature ranges anticipated in this study.

Note from Equation 14 that for convective cooling (when  $T_{air}$  is less than  $T_{cam}$ ),  $q_{c,a}$  is positive and for convective heating (when  $T_{air}$  is greater than  $T_{cam}$ )  $q_{c,a}$  is negative.

### 2.5.3.2 Determination of Significant Length

The significant length is the physical dimension over which convective heat transfer takes place. The geometrical shape and physical size of the incising pattern in the perfusion screen control the significant length. The incised pattern which is the repeated unit in the perfusion screen studied in this report, is pictured in Figure 32. The length  $d$  is the reference dimension and the three incised patterns prepared for this study have the same relative dimensions shown in Figure 32. The significant length is a weighted mean length, defined by (Ref. 1).

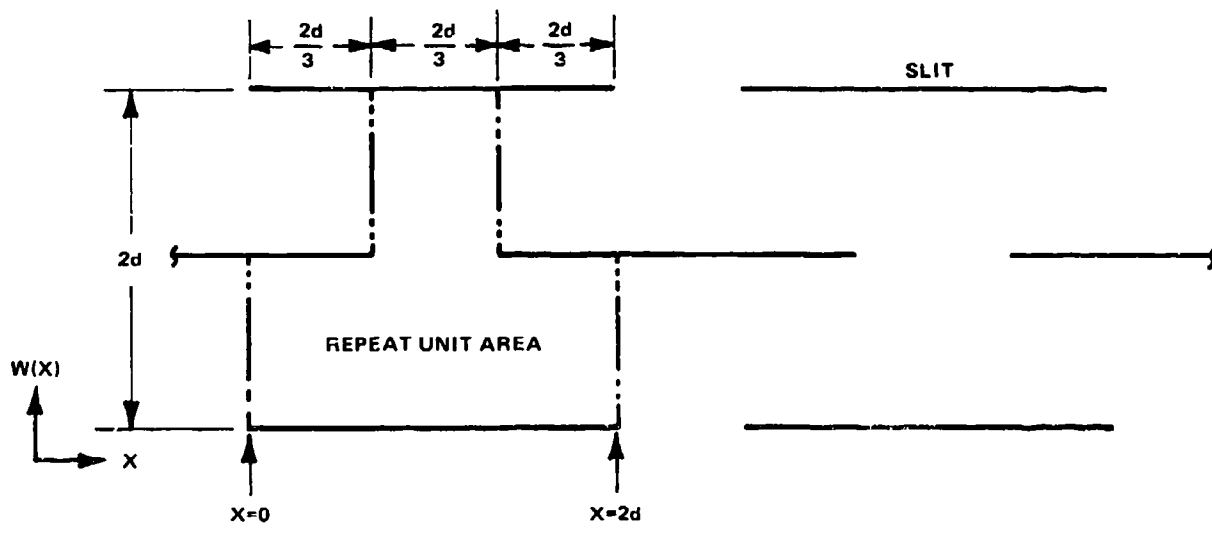
$$L = \frac{\int_0^{2d} w(x)^{\frac{1}{2}} dx}{\int_0^{2d} w(x)^{-\frac{1}{2}} dx} \quad (18)$$

where  $w(x)$  is the length in the direction of air flow and  $2d$  is the overall length of the incised pattern repeat unit. Integration of Equation (18) for the geometry shown in Figure 32 gives

$$L = 1.26 d$$

### 2.5.3.3 Perfusion Screen Convection Model

It is anticipated that Equation 14 will overestimate the heat transfer due to forced convection. This is because the perfusion air velocity flow over each incised unit in the perfusion screen is actually expected to be less than the free stream air velocity. Likewise the actual length dimension involved in forced convection heat transfer may differ from the calculated significant length. It is necessary, therefore, to take into account the air flow resistance of the



2218

Figure 32. Incised Pattern Repeat Unit for Perfusion Screen

perfusion screen and, in addition, our inability to directly measure the correct air flow velocity to be used in the convection term or to determine the appropriate significant length. Therefore, Equation 14 is modified to read

$$q_{c,a} = 2 K_c \sqrt{\frac{PV}{L}} (T_{cam} - T_{air}) \quad (19)$$

where  $P$  is defined as the perfusion factor.  $P$  is an empirical parameter which has to be determined for each incising pattern and geometry through field test measurements. We expect that  $P$  corrects mainly for the uncertainty in perfusion air velocity. A relatively minor influence on  $P$  is anticipated for the significant length dimension correction.

#### 2.5.4 Energy Balance Result

Assuming that the camouflage emissivity,  $\epsilon_{cam}$ , is equal to the thermal absorptance,  $\alpha_t$ , and using equations 9-11 and equation 19, equation 8 becomes

$$\begin{aligned} \alpha H + \epsilon_{cam} \sigma T_{sbb}^4 + \epsilon_{cam} \sigma T'_{gbb}^4 &= \\ 2\sigma T_{cbb}^4 + 2 K_c \sqrt{\frac{PV}{L}} (T_{cam} - T_{air}) \end{aligned} \quad (20)$$

Solving for  $\alpha H$ , and rearranging terms, we have

$$\begin{aligned} \alpha H &= 2 K_c \sqrt{\frac{PV}{L}} (T_{cam} - T_{air}) + \sigma (T_{cbb}^4 - \epsilon_{cam} T_{sbb}^4) \\ &\quad + \alpha (T_{cbb}^4 - \epsilon_{cam} T'_{gbb}^4) \end{aligned} \quad (21)$$

Assuming that the camouflage is a grey body and from the definition of emissivity, camouflage blackbody temperature is

$$T_{cbb}^4 = \epsilon_{cam} T_{cam}^4$$

The final form for the energy balance is therefore

$$\begin{aligned} \alpha H &= \underbrace{\text{solar heat}}_{\alpha H} + \underbrace{\text{convection}}_{2K_c \sqrt{\frac{PV}{L}} (T_{cam} - T_{air})} + \underbrace{\text{net radiation to sky}}_{\epsilon_{cam} \sigma (T_{cam}^4 - T_{sbb}^4)} \\ &\quad + \underbrace{\text{net radiation to ground}}_{\epsilon_{cam} \sigma (T_{cam}^4 - T'_{gbb}^4)} \end{aligned} \quad (22)$$

Thus, solar heat is balanced by convection to air, radiation to the sky, and radiation to the ground. Because these terms are dealt with individually later they are defined here as  $q_{r,s}$  for radiation to the sky and  $q_{r,g}$  for radiation to the ground. (Convection is already given in equation 19). Therefore

$$q_{r,s} = \epsilon_{cam} \sigma (T_{cam}^4 - T_{sbb}^4) \quad (23)$$

and

$$q_{r,g} = \epsilon_{cam} \sigma (T_{cam}^4 - T'_{gbb}^4) \quad (24)$$

In the perfusion screen equation (22), there is a parameter set characteristic of the screen material, design, and construction, and two physical constants. Table 1 lists the parameter sets. The perfusion factor P can be calculated after the remaining parameters are determined for a particular scenario. Because P is introduced as a semi-

TABLE 1  
PERFUSION SCREEN PARAMETERS

<u>Scenario</u>	<u>Perfusion Screen</u>	<u>Physical Constants</u>
$H$ [mW/cm <sup>2</sup> ]	$\alpha$	$K_c$ [mWsec <sup>1/2</sup> /cm <sup>2</sup> K]
$V$ [cm/sec]	$\epsilon_{cam}$	
$T_{air}$ [ K ]	$L$ [cm]	$\sigma$ [mW/cm <sup>2</sup> K <sup>4</sup> ]
$T_{sbb}$ [ K ]	$T_{cam}$ [ K ]	
$T_{gbb}$ [ K ]	P	

empirical parameter, the perfusion screen model is forced to be consistent with each set of field test measurements.

Once the energy balance terms for solar heat, and the two radiation terms are evaluated, the net heat exchange due to forced convection is determined. Using Equation (19), it is then possible to calculate  $P$  for each perfusion screen.

The scenario parameters used in the perfusion factor calculations are either measured directly or calculated from the test measurements. As discussed in the test measurement section (2.4) the solar irradiance  $H$ , the free stream wind velocity,  $V$ , and the radiometric blackbody temperature of the ground,  $T'_{gbb}$ , are measured directly. It was found more difficult to determine accurately the air temperature,  $T_{air}$ , and the appropriate blackbody temperature of the sky,  $T_{sbb}$ . Appendices B and C describe in detail how  $T_{air}$  and  $T_{sbb}$  are determined, respectively.

The perfusion screen parameters for solar absorptance,  $\alpha$ , and camouflage emissivity,  $\epsilon_{cam}$ , were determined from independent measurements. The methods used are discussed in Appendices C and D, respectively. Because a radiometric measurement is made for the camouflage, the actual camouflage temperature,  $T_{cam}$ , must be evaluated. Appendix A gives the method used to obtain  $T_{cam}$ . The method used to obtain the significant length,  $L$ , was presented in section 2.5.3.2.

### 2.5.5 Energy Balance Calculation for Obtaining Perfusion Factor

Once the energy balance terms are evaluated in Equation (22), the perfusion factor can be calculated. In order to show the method to obtain  $P$ , the data taken from the February 16, 1982 daytime test on the 1.0cm perfusion

screen is used. Table 2 presents parameter values used to determine the energy balance terms. Note that the radiometric blackbody temperatures of the sunlit ground and the shaded ground (short brown grass) represented the highest and lowest recorded values (see Figure 13). Because the perfusion screen shaded approximately half of the ground directly below, with the other half being sunlit,  $T'_{gbb}$  was taken as the median between the average shaded and average sunlit measurements. The individual energy balance terms are calculated below and P is determined.

#### Solar Absorption

The heat absorbed by the camouflage is

$$\alpha H = 0.67 \cdot 63 \text{ mW/cm}^2$$

$$\alpha H = 42.2 \text{ mW/cm}^2$$

#### Net Ground Radiation

Equation (4) gives net radiation to ground for these data as

$$q_{r,g} = 0.93 \cdot 5.67 \times 10^{-9} \frac{\text{mW}}{\text{cm}^2 \text{ K}^4} \{ (302.0 \text{ K})^4 - (298.7 \text{ K})^4 \}$$

$$q_{r,g} = 1.9 \text{ mW/cm}^2$$

The positive value indicates the camouflage is being cooled by the ground.

TABLE 2  
 PARAMETER VALUES FOR THE 1.0CM SCREEN  
 TAKEN ON 2/16/82

<u>Scenario</u>	<u>Perfusion Screen</u>	<u>Physical Constants</u>
$H = 63 \text{mW/cm}^2$	$\alpha = 9.67$	$K_C = 0.39 \frac{\text{mWsec}^{\frac{1}{2}}}{\text{cm}^2 \text{K}}$
$V = 198 \text{cm/sec}$	$\epsilon_{cam} = 0.93$	
$T_{air} = 293.9 \text{ K}$	$L = 1.26 \text{cm}$	$\sigma = 5.67 \times \frac{10^{-9} \text{mW}}{\text{cm}^2 \text{K}^4}$
$T_{sbb} = 272 \text{ K}$	$T_{cam} = 302.0 \text{ K}$	
$T_{gbb} = 298.7 \text{ K}$		

### Sky Radiation Term, $q_{r,s}$

Equation (23) gives net radiation to the sky. For these data,

$$q_{r,s} = 0.93 \cdot 5.67 \times 10^{-9} \frac{\text{mW}}{\text{cm}^2 \text{K}^4} \{ (302.0 \text{ K})^4 - (272 \text{ K})^4 \}$$

$$q_{r,s} = 15.0 \text{ mW/cm}^2$$

The positive value indicates the camouflage is being cooled by the sky.

### Forced Convection Term

Equation (22) can be solved for the forced convection term to give  $q_{c,a} = \alpha H - q_{r,s} - q_{r,g}$

Substituting the results calculated above

$$q_{c,a} = 42.2 \frac{\text{mW}}{\text{cm}^2} - 15.0 \frac{\text{mW}}{\text{cm}^2} - 1.9 \frac{\text{mW}}{\text{cm}^2}$$

$$q_{c,a} = 25.3 \text{ mW/cm}^2$$

The positive sign indicates that the camouflage is being cooled by forced convection. Note that 60% of the solar heat load is being dissipated by forced convection.

### Perfusion Factor

Equation (19) can be solved for the perfusion factor to give

$$P = \frac{L}{4K_c^2 V} \left( \frac{q_{c,a}}{T_{cam} - T_{air}} \right)^2 \quad (25)$$

Substituting parameter values, we have

$$P = \frac{1.26 \text{ cm}}{4 \left( 0.39 \frac{\text{mW sec}^{\frac{1}{2}}}{\text{cm}^2 \text{ K}} \right)^2 198 \text{ cm/sec}} \left( \frac{25.3 \text{ m W/cm}^2}{302.0 \text{ K}-293.9 \text{ K}} \right)^2$$

$$P = 0.10$$

#### Perfusion Factor Results From 2-16-82 Daytime Data

The 2/16/82 daytime test data was used to determine P for the three perfusion screens. Six separate measurements were made on each perfusion screen. P was calculated from each measurement according to the example given above. The six values were then averaged to give the final results, with the percent variation, presented in Table 3. The average of the energy balance terms is also presented with the percent of the total heat input dissipated by convection, sky radiation, and ground radiation.

#### Discussions of Relative Performance

The perfusion factor is characteristic of the particular perfusion canopy design and construction. Specifically the three designs used in this study are scaled by varying only the significant length, L. In addition, the forced convection coefficient, h, in terms of the model parameters is given by

$$h = K_c \sqrt{\frac{PV}{L}}$$

With the same free stream air velocity for the sample designs, the relative convection coefficients are given by  $\sqrt{L/L}$ . It is, therefore, suggested that the factor  $\sqrt{P/L}$  be used as the measure of relative performance.

TABLE 3  
 PERfusion FACTORS AND ENERGY BALANCE FROM  
 2/16/82 DAYTIME DATA

Perfusion Screen Row Separation, d	Perfusion Factor	Energy Balance Terms			
		Solar Load mW/cm <sup>2</sup>	Convec- tion mW/cm <sup>2</sup>	Radiation to sky mW/cm <sup>2</sup>	Radiation to ground mW/cm <sup>2</sup>
0.5 cm	0.045 ± 60%	40.9	23.9 (58%)	15.0 (37%)	1.9 (5%)
1.0 cm	0.10 ± 40%	40.9	24.9 (61%)	14.6 (36%)	1.5 (4%)
2.0 cm	0.23 ± 60%	40.9	24.8 (61%)	14.7 (36%)	1.6 (4%)

The following table summarizes the relative performance from the February 16, 1982 test data.

Perfusion Screen Row Separation, d	L [cm]	P	P/L [cm <sup>-3</sup> ]
0.5 cm	0.63	0.045	0.27
1.0 cm	1.26	0.10	0.28
2.0 cm	2.52	0.23	0.30

The relative convection coefficients are the same, within the accuracy of the test measurements as seen by the closeness of the terms in the last column.

This result is consistent with camouflage temperature results. The average camouflage temperatures from the February 16, 1982 experimental data are:

Perfusion Screen Row Separation, d	T <sub>cam</sub> (average) [K]	T' <sub>cbb</sub> (average) [K]
0.5 cm	302.0	300.2
1.0 cm	301.3	299.5
2.0 cm	301.4	299.6

Note that although the T<sub>cam</sub> values are approximately 7 to 8 degrees above air temperature (T<sub>air</sub> = 294 K), the radiometric blackbody temperatures are all within 1.5 degrees of the radiometric blackbody temperature of the ground (T'<sub>gbb</sub> = 298.7 K).

### 3.0 DISCUSSION

#### 3.1 CS-86 Compatibility.

One of the objectives of this contract was to make an evaluation of the perfusion screen as a viable component of the Modular Multispectral Camouflage System 1986 (CS-86). This system is understood to include the following objectives. The CS-86 camouflage should:

- 1) be applicable to all Army tactical systems
- 2) be applicable to moving as well as stationary targets
- 3) defeat sensors in all wavebands
- 4) defeat laser designators and rangefinders
- 5) have modularity
- 6) have all-season capability

It is helpful to consider first the methods of achieving the above CS-86 goals. Goals 1, 2, and 5 appear to be concerned with camouflage overall system design (such as canopy or disrupter) and are not at the component level of interest of this contract. Viability of the perfusion screen concept as a component of CS-86 is regarded, therefore, to hinge primarily on the potential of this concept to meet goals 3, 4, and 6. Considering non-thermal wavebands, all of these goals are achievable through reflectance control which has been accomplished to a large extent with coatings. For the visual screen there is also the creation of texture and shadowing through leafy garnishment on netting but colors remain fundamental. Therefore, the issue of compatibility of the perfusion screen approach with CS-86 objectives centers on the interrelationship between surface coatings (to meet goals 3, 4, and 6) and thermal concealment performance.

The parameters related to material reflectance which also affect thermal performance as the heat balance equation in section 2.5.1, (22), shows are solar absorptance and material emissivity. Radar scattering material presently used in nets has no effect on surface reflectance in the .4 to 14 micrometer region. It may be assumed that it can be used with the perfusion screen also without any problem.

Figure 33 is a reflectance curve which represents what may be the desired camouflage reflectance to simulate natural foliated background. Notches in the curve represent special coating for laser absorption. Hopefully these notches can be made narrow enough so that the broad spectrum reflectance is only slightly affected and broad spectrum sensors continue to see about the same energy reflected as from the background.

Solar absorptance is a term which is closely tied to this curve because of the conservation of energy relation

$$\alpha + \rho + \tau = 1$$

where  $\alpha$  = absorptance

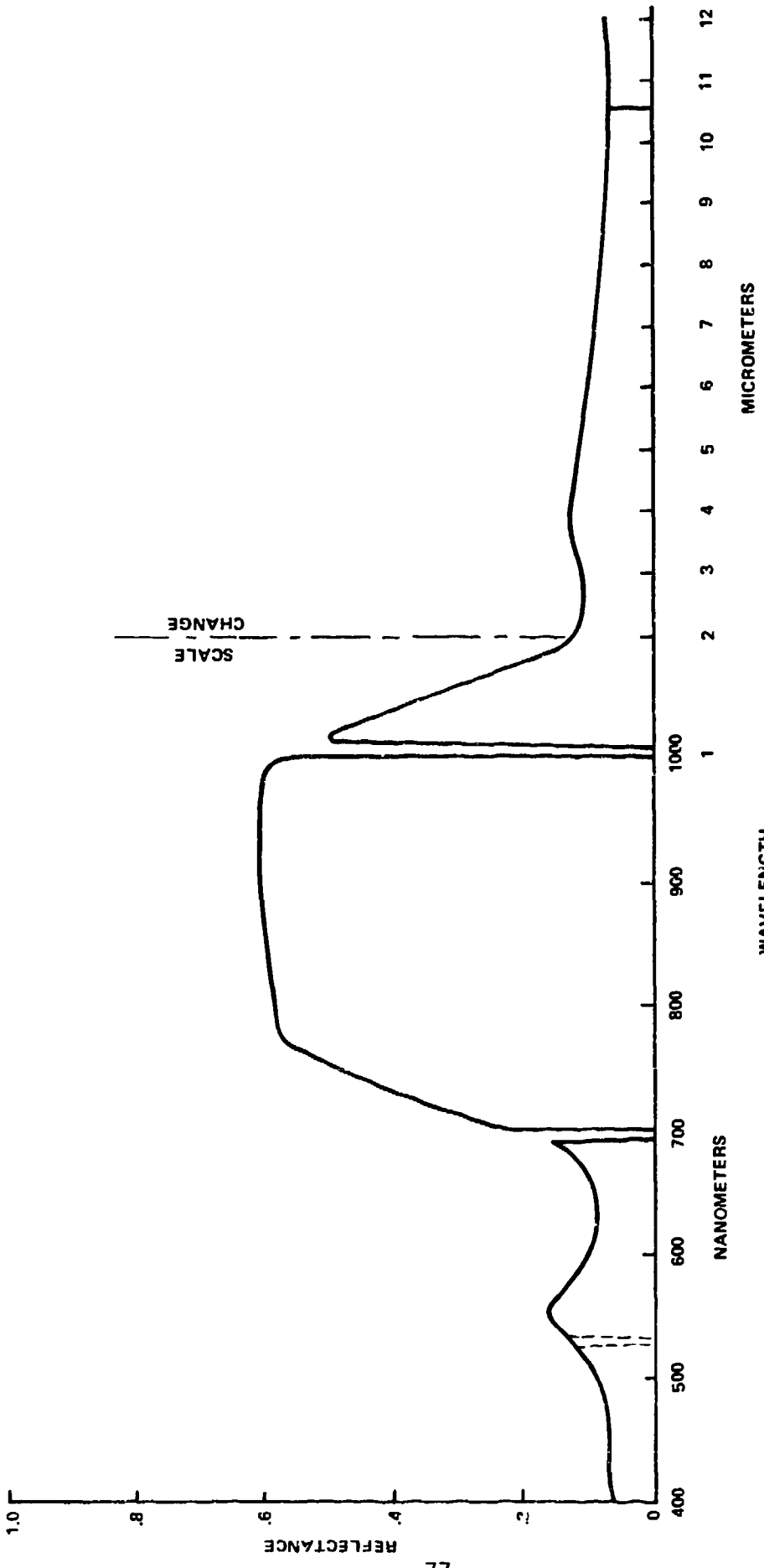
$\rho$  = reflectance

$\tau$  = transmittance

When  $\tau = 0$  (usually the case), then  $\alpha = 1 - \rho$ , so colors affect solar absorptance and consequently the temperature of camouflage materials in the daytime.

2219

Figure 33. Reflectance Curve Desirable for Camouflage



Compatibility with this kind of reflectance curve seems good for conditions of low cloud cover. In instances in which there was high cloud cover and yet sunlight was shining on the perfusion screens, they tended to temperatures at the upper end of those in the background and sometimes a little higher. That was with forest green paint coloration. Therefore, there may be a problem with maintaining color and keeping solar absorptance at a lower level so that solar heating is reduced for the perfusion screens. Further consideration to this subject is given in the following section on recommendations.

It is anticipated that the laser absorption notches in the reflectance curve will have negligible effect on solar absorptance or on emissivity. Laser rangefinder and designator absorption filtering is also not anticipated to cause any incompatibility problems for the perfusion screen.

### 3.2 Difficulties of the Perfusion Screen

Some problems were experienced with the perfusion screen in achieving the correct opening of layers. When a sheet was slit and the attempt was made to expand it, non-uniform opening occurred. Some of the slit elements opened one way and others opened the other way. For blocking cooperation between layers which leads to total blocking with two layers, all slit elements must open one way. That was accomplished in making test samples by manually forcing all elements to open in the same direction - sometimes slit by slit - a laborious procedure. Nevertheless, that is not regarded as a long range problem as manufacturing techniques should be able to overcome this problem.

There is some directionality in the appearance of the perfusion screen samples prepared. That is due to the uniform direction of opening on the exposed layer. Photographs of the samples indicate some effect but the color change still does not seem stark enough to be a problem. In fact, if the perfusion screen were used in pieces oriented in different directions as in a disrupter, the difference in darkness might be a help in increasing disruption and creating mottling even though the same color coating were on all perfusion screen sections.

Another difficulty which has been experienced with the perfusion screen embodiments is maintaining the degree of expansion which is desired to get good perfusion yet retain blocking effectiveness. Material elasticity tends to cause the sheets to relax to the unexpanded state. It was observed with screens made from the camouflage cloth used in the visual nets that the degree of stiffness was low and elasticity of the slit sheets high so that they had to be held in a stretcher frame to keep the expansion desired. However, after several days in the frame, the material seemed to have taken a set which maintained shape. It would still slowly relax though.

If a perfusion screen section were used in a camouflage device, some arrangement will be necessary to keep the section in the proper expansion - not too little so that it restricts perfusion and allows overheating in the sun or possibly overcooling at night, and not too much so that blocking is incomplete allowing some target radiation to escape directly.

This might be accomplished with attachment of the perfusion screen sections to netting which is then pulled square.

Another way might be to simply use materials in the construction of the perfusion screens which are stiff enough to retain shape on their own. Heat set mylar was mentioned in the materials analysis section of the investigation because of its heat settable property.

One of the difficulties anticipated in use of the perfusion screen concept relates to its use as a full canopy. The degree of air passage through the screen when it is of large extent is unknown. Test samples were about a half meter on a side and were tested in a horizontal position. Air was free to pass under and over the screen sections. In a full size canopy arrangement, this flow would be affected; and it is not known just what the thermal effect would be. Therefore, the testing actually simulated the case of a disrupter employment more exactly than a canopy.

### 3.3 Surface Garnishmen.

Because of the small scale regularity required to attain line of sight blocking with the perfusion screen, there may be an appearance of uniformity to the eye. A form of visual texturing could be achieved by laying visual garnishment on top of the screen. If it should be found that such a visual garnishment layer becomes too hot or cold, doubly incised garnishment can be used. This would be material with slits cut into it and expanded. Then in the expanded state it would be incised once more with the large visual incising cuts and expanded. The slit expanded material would just serve in the place of flat material so that the resulting garnishment would be more porous and would come to a thermal equilibrium temperature closer to air temperature than the standard visual garnishment. This is also discussed in the patent application for the perfusion screen.

## 4.0 CONCLUSIONS

### 4.1 Thermal Suppression Requirements and Thermal Load.

The thermal suppression requirement study produced several conclusions. First, the most exact thermal requirement for camouflage is that the equivalent blackbody temperature of the camouflage fall within some vicinity of the background within the naturally occurring range of the background within some vicinity of the camouflage. This, however, is not quantitative. To quantify the requirement, it was concluded that a rule-of-thumb is that camouflage equivalent blackbody temperatures need to be within from  $\pm 2$  to  $\pm 7^{\circ}\text{C}$  of average background temperature, depending on the environmental condition. The most restrictive condition was expected to be just pre-dawn and the least in the day in bright sun.

One of the conclusions concerning the case of unresolved targets was that long range detection avoidance may be possible without the necessity of reducing target temperatures as low as the background temperatures.

The spatial or patterning requirement was for a thermal pattern with smallest lobes in an irregular pattern on the order of 20 inches across.

The angular coverage analysis, though not extensive, indicated possible gain from terrain masking so that camouflage need not provide full hemispheric coverage which was felt to be needed otherwise. Terrain masking may allow generally a 1 to 5 degree region above the horizontal to be uncamouflaged.

It was concluded that thermal load for targets can be reduced to one basic parameter - target surface temperature. Most targets have surface temperatures (on surfaces to which a perfusion canopy would be applicable - not engine exhausts for example) which differ from air temperature by the following maximum values:

Daytime	30-40°C
Night	25-30°C

The significance of these values is that if a camouflage method is capable of handling such levels of temperature difference with air temperature, it should be capable of covering the majority of target items.

Now it should be mentioned once more that the above conclusions on both thermal suppression requirement and on thermal load were not arrived at to represent finalized performance criteria: rather they are in the nature of working definitions.

#### 4.2 Thermal Suppression Performance.

Conclusions regarding the thermal suppression of perfusion canopy samples were drawn from temperature tests (with a radiometric thermometer instrument) and from imaging tests in which both the radiometric thermometer and a thermal imager were used.

##### 4.2.1 Night Performance.

The night tests were sparse (two nights), but results were good both times. The conclusion is that the night condition is compatible with good matching of the perfusion canopy with background elements. There was no overcooling evidenced at all so none would be expected based on these tests.

#### 4.2.2 Day performance.

The perfusion screen canopy samples showed a dependence on the environmental condition existing at the time of the test. Basically what was noted was the adequate performance of the test samples in sun provided the cloud cover was low. In a condition of high solar load and simultaneously high cloud cover, the perfusion canopy samples drifted up to the upper end of the background variation and sometimes beyond. Performance in a high solar, high cloud cover condition is therefore regarded as marginal. In a low solar load, high cloud cover condition, performance may again be anticipated to be satisfactory.

One objective was to make a performance determination between the three different sizes of perfusion canopy sample which had been prepared. The conclusion reached after the test series is that there is no significant difference between the three in thermal performance. There was indication in analysis of the radiometric temperature testing that the largest size (2 cm slit row separation) was slightly superior to the other two sample sizes.

It was the conclusion in fact from analysis or radiometric temperature test results that convection from each of the three samples is about the same. This comes from the observation that the  $\sqrt{P/L}$  value (that part of the convection term depending on the sample) for the three samples was nearly constant contrary to expectation. The smaller sample was expected to afford better convection because perfusion was expected to be about the same for all samples. That is, the relative wind through each size perfusion screen was not expected to change with the size of the screen, which the results indicate it did. If convection is about the same for all three sizes of screen, the size choice, from the present data anyway, would

be for the largest one, the 2cm slit row separation (4cm slit width) sample.

#### 4.2.3 Miscellaneous Conclusions.

From hot plate testing, several conclusions can be drawn. First though elementary, the sample screens did not transmit infrared radiation in the 8-14  $\mu\text{m}$  region directly. Second, a spacing of about 6 inches was adequate to negate the influence of a hot plate some 28°C warmer than air. That was true for the screen parallel to the hot plate whether the arrangement was vertical or horizontal. That was observed in both day and night tests. This is a tentative conclusion for small target and canopy size, but it is a hopeful indicator for application of the perfusion canopy to bigger targets. It suggests that extreme spacing will not be needed for proper dilution cooling of air heated by passing over target hot surfaces.

Tests of the perfusion screen samples in a vertical orientation were conducted and it was concluded that generally little thermal effect may be anticipated due to vertical orientation, as opposed to horizontal. That may not be true when the orientation is from horizontal to a condition normal to sunlight and parallel to the wind direction.

Another conclusion which came from the tests was that thermal mottling can be obtained by the addition of garnishment on top of a perfusion screen. It is not, however, a strong mottling as observed but does indicate the potential for enhancing thermal effectiveness with surface garnishment.

#### 4.3 CS-86 Component Viability.

The overall conclusion which can be made considering all the above is that the perfusion canopy concept does offer

a means of thermal concealment which does not overheat in solar load nearly to the degree which thermal blankets do and is in many cases within the background variation in equivalent blackbody temperature. Assuming matters of production and storage can be solved, the perfusion screen is compatible with laser and radar suppression requirements in that coatings to achieve those effects can be added without impact on thermal performance of the perfusion screen. Colors chosen to achieve visual camouflage will impact thermal performance due to their influence on solar absorptance,  $\alpha$ . The indication here is that  $\alpha = .7$  (the indirectly measured value for the forest green paint used) is a little too high.

Noting that a lower value of solar absorptance would probably best suit thermal performance of the perfusion canopy, it still appears reasonable to conclude that the perfusion canopy is compatible with the visual camouflage requirements as well as with radar and laser suppression methods. Performance in the night appears to be good at this point and the response to solar load, though not at an optimum, is still a marked improvement over that of the thermal blanket. Therefore, it is concluded that the perfusion canopy concept gives indications that it is a viable candidate to assume some of the responsibility of the CS-86 system.

## 5.0 RECOMMENDATIONS.

Because of the marginal performance of the perfusion canopy in some daytime conditions (high solar, high cloud cover), it is recommended that consideration be given to development of a paint which reduces solar load. That can be done without sacrificing visual performance by proper selection of transmitting, reflecting and absorptance properties of the coating. What is suggested here is to decrease solar absorptance and increase transmittance while keeping reflectance at about the same level as for required visual/near IR performance. Leaves naturally have such solar transmission. Paints and coatings on the other hand, tend to be opaque so that they will have good "hiding power" or cover in a few coats. In this case that is undesirable. What is needed is an integrated coating/substrate analysis to define the system reflectance in terms of individual part reflectance, absorptance, and transmittance. Then this method of analysis can be used to determine the anticipated reflectance of various combinations of paint/coating and substrate and the reduction in solar load which can be obtained.

Future examination of the perfusion canopy should include more detailed determination of the effect of orientations other than horizontal. In particular the case (expected to be worst) of canopy normal to the sun and parallel to the wind in a high cloud cover ambient would be of interest to explore the limits of performance - how high temperatures for the perfusion canopy might get.

It was noted that in earlier testing of the perfusion canopy the background against which it was tested was dry brown grass due to the season of the year. Later on when

spring arrived the greening of the background may have resulted in greater differences between the perfusion canopy and background. That suggests that other backgrounds should be found against which to test. It is recommended that a sandy background, a green grass background, and a rocky background be sought and tests conducted to note the degree to which perfusion canopy samples fit into those background variations.

As a method of comparison to known data, it is also recommended that a small visual screen sample be included in testing with the samples of perfusion canopy.

In order to more realistically assess performance it is recommended that larger size perfusion screens be made and tested. Probably they should be made in 2 cm slit width in the proportions described in this report (figure 4 (b)). A suggested dimension is 1 meter squares. Five such squares could be used in concert to cover an actual target. Together with the work to make the screens some effort will be needed to design a method of support for the screens. These screens tend to collapse when the stretching force is removed as they are presently made. That is the reason why they were fastened into stretcher frames for handling; that problem needs attention in future development.

When these larger screens and attendant support systems (possibly a disrupter form) have been assembled, tests should be conducted to evaluate the thermal suppression performance of the perfusion canopy on an active and a passive target (one generating heat and one not). A passive target might be just a small car with dark color if possible, or even better, a jeep and an active target might be a small generator.

Particular attention should be paid during the active testing to whether dilution cooling of air around the target is able to reach acceptable levels within a distance reasonable for spacing the perfusion screen away from the target.

Another objective of testing with larger sections of perfusion screen would be to note the effect of increasing scale - to observe whether large size pieces behave in a similar way to what the smaller ones already tested did.

In order to investigate mottling further it is recommended that garnishment for addition to the surface of the large pieces of perfusion screen be procured and observed during testing.

## REFERENCES

1. Parkhurst, D. F. et al, "Convection Heat Transfer From Broad Leaves of Plants", Journal of Heat Transfer, Trans. ASME, vol. 90, series C, no. 1, Feb. 1968
2. Holman, J. P., Heat Transfer, 4th ed, McGraw-Hill, New York, 1976

APPENDIX A. ACTUAL TEMPERATURE FROM RADIOMETRIC BLACKBODY TEMPERATURE (MEASURED WITH R2LT)

The Raytek model R2LT radiometric thermometer was used in field tests to obtain readings from which actual surface temperatures were derived. The instrument was set to an emissivity of 1.00 so that a blackbody temperature would be read. The instrument actually indicates a temperature which corresponds to the total power received on its detector. That comes from two sources in reality and not just the emitted power from the surface at which the instrument is aimed. There is also a reflected power from the spot in view which boosts the indicated blackbody temperature above actual blackbody temperature. For the purposes here horizontal surfaces are the ones of interest so the source of reflected power is the sky.

This relationship can be expressed mathematically as

$$T'_{bb} = \left( T_{bb}^4 + \rho T_{sbb}^4 \right)^{\frac{1}{4}} \quad (A1)$$

where:

$T'_{bb}$  = radiometric blackbody temperature (indicated)

$T_{bb}$  = true blackbody temperature

$\rho$  = surface reflectance

$T_{sbb}$  = blackbody temperature of sky

Since most surfaces are opaque to thermal infrared (transmission at infrared wavelengths is zero), it is possible

to express surface reflectance as one minus absorption (from conservation of energy). Applying Kirchoff's law (emissivity = absorptance) assuming the surface is a gray-body, surface reflectance becomes

$$\rho = 1 - \epsilon$$

where:

$\epsilon$  = surface emissivity

Then radiometric or indicated blackbody temperature temperature is expressible as

$$T'_{bb} = \left[ T_{bb}^4 + (1 - \epsilon) T_{sbb}^4 \right]^{\frac{1}{4}} \quad (A2)$$

Therefore, to get actual surface temperature,  $T$ , from the indicated blackbody temperature by the radiometer, one needs to remove the reflected power to get true blackbody temperature and then divide out the surface emissivity and take the fourth root;

$$T = \left[ \frac{T'_{bb}^4 - (1 - \epsilon) T_{sbb}^4}{\epsilon} \right]^{\frac{1}{4}} \quad (A3)$$

Since blackbody temperature is needed in the thermal model for radiant cooling, testing already needs to assess a value for sky blackbody temperature. Thus it is already a term which is available for making this correction.

A point which should be observed is that the above equations are specifically directed toward horizontal surfaces. If measurement is made radiometrically with

the R2LT on vertical surfaces, then this correction will not be as helpful because approximately half of the reflected power will then come from the ground. For the present work only horizontal surfaces are considered.

## APPENDIX B. RADIOMETRIC MEASUREMENT OF AIR TEMPERATURE

The perfusion screen is based on the idea of convective coupling to air temperature as a means to control screen temperature difference with background. Therefore, a good knowledge of difference in actual screen temperature and air temperature is needed to assess the convective heat transfer from the screen.

Screen temperature is best measured radiometrically because it is a non-contact measurement. Radiometric measurement does not perturb screen temperature as contact means are likely to do. But a problem arises in that air temperature itself cannot be measured directly radiometrically because air is not a solid. It is readily measured with a mercury bulb thermometer, but any systematic error in either radiometric or mercury bulb devices can introduce that error into the temperature difference measurement needed for convection calculation.

Therefore, it was decided to create a device which would maintain a surface at air temperature which could then be read radiometrically. Figure B1 shows the resulting device.

The air vane material was chosen to be the same as that used for the perfusion screen samples so that the emissivity would be the same. Vanes were also situated on the inlet side of the fan so that any fan heating from the motor would not be added to the air passing through the air vanes to cause incorrect air temperature measurement.

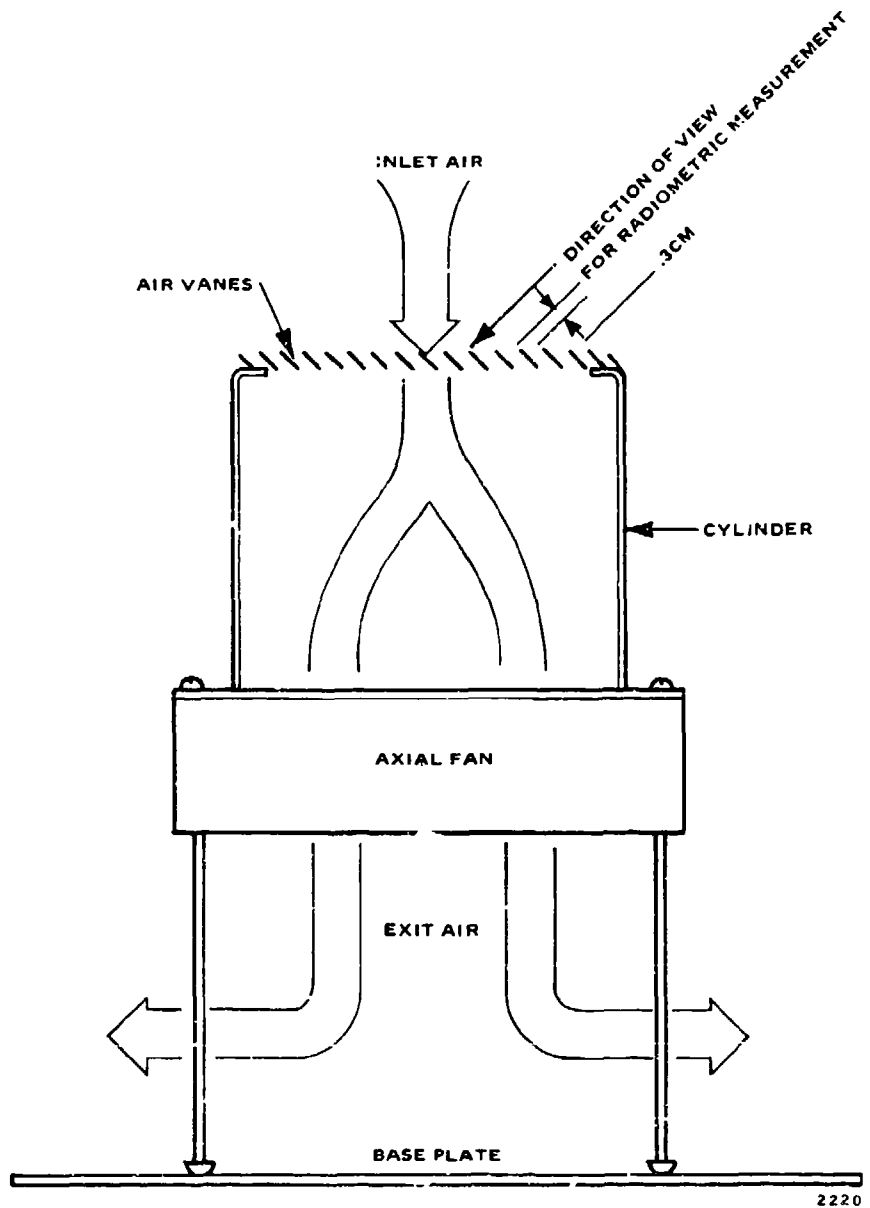


Figure B1. Device for Radiometric Measurement of Air Temperature

The equation for convection from the air vanes is basically the same one for convection from the perfusion screen - namely

$$q_{c,a} = 2K_c \left( \frac{V}{L} \right)^{\frac{1}{2}} (T_{av} - T_{air}) \quad (B1)$$

where:

$$K_c = .39 \text{ mW sec}^{\frac{1}{2}} / (\text{cm}^2 \text{ }^\circ\text{C})$$

V = wind through the vanes, cm/sec

L = significant length of air vanes, cm

T<sub>av</sub> = air vanes temperature

T<sub>air</sub> = air temperature

For the air vanes, a slit row separation of 0.3 cm was used. In section 2.5.3.2 where significant length is discussed, it was shown that significant length for the geometry of the perfusion screen layer was 1.26 times slit row separation. Using the same estimate of significant length for the air vanes, L = 0.38 cm.

With a hot wire anemometer (Datametrics model 100VT) the wind speed through the air vanes, at a point just under the air vanes inside the cylinder, was determined to be about 800 cm/sec.

Equation (B1) with the above values for a 10 mW/cm<sup>2</sup> net radiant load on the vanes predicts a temperature difference with air of about 0.3°C would occur. This is about the radiant load experienced in the daytime and nighttime testing.

Therefore, the magnitude of error in actual air temperature of the air vanes was taken to be about  $0.3^{\circ}\text{C}$  which was not regarded to be significant enough to take into account in calculations.

The procedure was then to measure the air vanes black-body temperature with the radiometric thermometer making sure that the direction of view was as indicated in Figure B1 so that only the air vanes were seen and not objects behind. This measurement was then corrected for reflected power from the sky as discussed in Appendix A.

## APPENDIX C. ASSESSMENT OF EFFECTIVE BLACKBODY TEMPERATURE OF SKY AND SOLAR ABSORPTANCE FOR FOREST GREEN PAINT

### 1.0 EFFECTIVE BLACKBODY TEMPERATURE OF SKY

In the heat balance for an element of a horizontal perfusion screen, radiant cooling to the sky has been found to be a strong influence. In addition, the direct measurement of sky temperature radiometrically with the Raytek R2LT is not feasible because this instrument operates in the 8-14 micrometer region which happens to be an atmospheric transmission window. Therefore, the radiometric temperature read by the R2LT is excessively low because radiant emission in the atmospheric windows is low. In the whole spectrum exchange probably most of the radiant influence of the sky comes from the absorption bands. Another method of assessing an effective sky temperature for radiant cooling was needed.

It was determined that an indirect measurement could be made by using a white insulated pad laid on the ground and shaded. The temperature of this pad is measureable with the R2LT. Furthermore the heat balance for the pad is predominantly controlled by sky temperature.

This method circumvented the problem of direct measurement of equivalent blackbody temperature of the sky. Instead, the pad temperature was measured after allowing real radiant exchange processes involving spectral variation in atmospheric absorption through the whole spectrum to govern the white pad temperature. Then, the results were put into an equation for the heat balance as if the sky cooling were a whole spectrum radiant exchange between graybodies.\* In this way, an effective blackbody temperature of the sky was obtained. Then it was assumed that this effective sky temperature could be used in the heat balance equation for the perfusion screen (equation (22)

---

\* A graybody is one for which the emissivity is spectrally invariant.

of the main text) in the sky radiation term, which was also set up as a graybody exchange.

Equation (C1) gives the heat balance for the pad, showing cooling to the sky as a graybody exchange balanced by convection, diffuse solar heating and conductive heating.

$$\underbrace{\sigma(T_{pbb}^4 - \epsilon_p T_{sob}^4)}_{\text{Sky Cooling}} = \underbrace{K_c \left(\frac{V}{L}\right)^k (T_{air} - T_{pad})}_{\text{Convection Heating}} + \underbrace{\alpha_p H_d}_{\text{Solar Heating}} + \underbrace{\frac{k}{t} (T_g - T_{pad})}_{\text{Conduction Heating}} \quad (C1)$$

where:

$\sigma$  = Stefan-Boltzmann Constant,  $5.67 \times 10^{-9} \text{ mW}/(\text{cm}^2 \text{K}^4)$

$T_{pbb}$  = Blackbody temperature of pad surface, K

$\epsilon_p$  = white pad surface emissivity

$T_{sob}$  = blackbody temperature of sky, K

$K_c$  = forced convection factor,  $.39 \text{ mW sec}^{1/2}/(\text{cm}^2 \text{K})$

V = ambient wind speed, cm/sec

L = significant length for pad surface, cm

$T_{air}$  = air temperature, °C

$T_{pad}$  = pad surface temperature, °C

$\alpha_p$  = white pad surface solar absorptance

$H_d$  = diffuse solar irradiance

$$\begin{aligned}
 k &= \text{pad insulation thermal conductivity, mW/(cm K)} \\
 t &= \text{pad thickness (insulation), cm} \\
 T_g &= \text{ground temperature under pad, } ^\circ\text{C}
 \end{aligned}$$

The pad was surfaced with a piece of white bond paper to minimize solar heating during the day. The procedure of shading was also to minimize that term. Conduction can then be made comparatively quite small through the use of several inches of insulation. The dominant influences are thus sky cooling and convection when these steps have been taken.

Equation (C1) can be solved for  $T_{sbb}$  as

$$T_{sbb} = \left\{ \frac{1}{\varepsilon_p \tau} \left( \alpha T_{pbb}^4 - K_c \left[ \frac{V}{L} \right]^{\frac{1}{2}} (T_{air} - T_{pad}) - \alpha_p^H d \frac{k}{t} (T_g - T_{pad}) \right) \right\}^{\frac{1}{4}} \quad (C2)$$

Quantities to the right in (C2) are either known or measurable or can be estimated with sufficient accuracy to permit a first calculation of  $T_{sbb}$ . However, because sky temperature itself influences to a degree some of the quantities in the right side of (C2), it was necessary to iteratively solve for  $T_{sbb}$ .

Appendix A shows that radiometrically measured temperatures of surfaces should be compensated for the effect of sky temperature. Therefore,  $T_{pad}$  and  $T_{pbb}$  as measured directly with the radiometric thermometer, need correction for  $T_{sbb}$  for best accuracy. Furthermore,  $T_{air}$  measured indirectly as the radiometric temperature of air vanes is also influenced by sky temperature in the same way. This is discussed in Appendix B.

A workable iteration to solve for sky temperature is to use air temperature measured with a mercury bulb thermometer in (C2) to get an estimate of sky temperature and use this estimate to correct pad temperature and air vanes temperature. Then these two new values of pad temperature and air temperature will yield a new sky temperature. After one or two such iterations, sky temperature generally ceases to change significantly and the resulting values for both sky blackbody temperature and air temperature from the air vanes are available for use in the model.

#### Example Calculation of Sky Temperature

An example of this procedure is presented here using data from a test conducted in the day on 2-16-82. A programmable calculator was used to perform the iteration.

Input data were:

pad temperature measured, $T'_{\text{ppb}}$	14°C
assumed solar absorptance, $\alpha$	0.15
solar irradiance, diffuse, $H_d$	9.4 mW/cm <sup>2</sup>
assumed paper emissivity, $\epsilon_p$	0.95
ground temperature under pad, $T_g$	18.7°C
average wind speed, $V$	245 cm/sec
pad significant length, $L$	49 cm
air temperature, Hg bulb	22.5°C

Sky blackbody temperature varied in the following way as the iteration proceeded: 285.8K, 275.2K, 276.6K. The variation in temperature between the last two calculations of sky temperature was not regarded as significant so the iteration was terminated and the sky temperature was taken to be 277K.

## 2.0 SOLAR ABSORPTANCE FOR FOREST GREEN PAINT

In a manner quite similar to that used to get effective blackbody temperature of the sky, it is possible to get an estimate of the solar absorptance indirectly from measurements made on an insulated pad surfaced with the material whose solar absorptance it is desired to get. In this case, what was done was to paint a sheet of spunbonded polyolefin with the same forest green paint used on the perfusion screen samples and affix it on one side of the same insulated pad used for sky temperature calculation. Thus, except for the effects produced by slitting and expansion, the sheet solar absorptance should be the same as for the perfusion screen samples because the materials were identical.

The heat balance equation for this case is identical to that for sky temperature calculation (equation C1), with the exception that solar irradiance is total - not just diffuse as for the sky temperature measurements. That is because the green sheet must not be shaded, of course, when it is the solar absorptance which is of interest. The applicable equation used in determination of solar absorptance,  $\alpha$ , was

$$\alpha = \frac{1}{H} \left[ \sigma(T_{pb}^4 - \epsilon_{gp} T_{sb}^4) + \frac{k}{t} (T_{pad} - T_g) + K_c \left( \frac{V}{L} \right)^{\frac{1}{4}} (T_{pad} - T_{air}) \right] \quad (C3)$$

where:  $H$  = total solar irradiance

$T_{pb}$  = green pad surface blackbody temperature

$\epsilon$  = green pad emissivity

$T_{pad}$  = green pad surface temperature

Other quantities are the same as in (C1).

The procedure in the absorptance measurement was to first make a sky temperature measurement set as discussed earlier. Then the pad was turned over (the green surface was on the opposite side of the pad from the white surface used for sky temperature measurement) and allow it to come to equilibrium for about five minutes. Then pad surface temperature was measured simultaneously with an averaging of wind speed. The pad was raised briefly while a quick measurement of ground temperature was taken and solar irradiance noted (meter parallel to the pad). As for sky temperature, a measurement of air vanes temperature. (Appendix B) was also made.

#### Measurement Results

On February 16, 1982, a set of measurements as described above was made. Table 1 gives the measurements and results of calculation for  $\alpha$  for  $L = 49\text{cm}$ ,  $T_{\text{sky}} = 272\text{ K}$ ,  $T_{\text{air vanes}} = 20.6^{\circ}\text{C}$ ,  $K_C = .39 \text{ mW } \sqrt{\text{sec}} / (\text{cm}^2 \text{ }^{\circ}\text{C})$ ,  $H = 57 \text{ mW/cm}^2$ .

The solar absorptance results from this testing suggest that the forest green paint on spunbonded polyolefin as was used for the perfusion screen samples was about 0.67. Since this is an indirect measurement, it is expected that it may be in error by perhaps .05.

TABLE 1. SOLAR ABSORPTANCE CALCULATION FOR FOREST GREEN PAINT

$T'_{pbb}$	Net Rad. Cool	$T_{pad}$	$T_g$	Cond. Cool	V	Conv. Cool	$\alpha$
°C	mW/cm <sup>2</sup>	°C	°C	mW/cm <sup>2</sup>	cm/sec	mW/cm <sup>2</sup>	
39.1	22.90	41.57	21.4	1.55	166	15.07	.69
35.5	20.46	37.78	20.7	1.31	238	14.77	.641
36.6	21.18	38.94	21.0	1.37	240	15.83	.67
			(avg.			(avg.	
			last			last	
			two)			two)	

For  $L = 49$  cm,  $T_{sky} = 272K$ ,  $T_{air vanes} = 20.6^\circ C$

$$K_C = .39 \text{ mW } \sqrt{\text{sec}} / (\text{cm}^2 \text{ }^\circ\text{C}), H = 57 \text{ mW/cm}^2$$

#### APPENDIX D. EMISSIVITY MEASURFMENT ON FOREST GREEN PAINT

Because the perfusion screen samples were made with a forest green paint for visual effect, it was also necessary to determine the surface emissivity of this coating for model calculations. The following procedure was conducted to make an evaluation of this emissivity.

A Thermolyne model HPA1915B hot plate was spray painted with forest green paint (made to meet MIL-E-52798A (ME) type II) and used as the test surface. In order to monitor the surface temperature of the hot plate, a 1.5 x 1.0 inch x about 4 inch long bar of aluminum was drilled out to clear a mercury bulb thermometer so that it could be inserted into the bar up to the immersion line. The hole was first filled partially with Dow-Corning heat sink compound. The bar was then heat sunk to the hot plate surface with the same compound and insulated on 4 sides with 3/4 inch thick urethane foam insulation.

Hot plate temperature was not contrclled by the knob, but was controlled by setting the knob full on and reducing the voltage to the hot plate with a Variac (setting 20). In this way a more stable temperature was attained after sufficient time.

The surface temperature was then measured radiometrically with the Raytek Model R2LT thermometer. Emissivity was determined by adjusting the radiometric reading with the emissivity setting on the R2LT until the radiometric reading was equal to the mercury bulb reading.

The results of this are shown in Table D1.

TABLE D1. EMISSIVITY MEASUREMENT

Date	H <sub>g</sub>	Bulb	$\epsilon$	T' <sub>bb</sub> ( $\epsilon=1$ ) (radiometric blackbody)
2-3-82	58.6		.93	
			.93	58.8
2-4-82	40.0		.91	38.3
			.92	

It was felt that the value 0.93 was probably the most correct emissivity for the forest green paint. It should be noted that this is an 8-14  $\mu\text{m}$  emissivity, since that is the response band of the R2LT thermometer.

APPENDIX E. INFRARED IMAGER SPECIFICATIONS

INFRAMETRICS MODEL 525

Temperature Measurement Range	-20°C to 1500°C
Minimum Detectable Temperature	0.2°C
E-O Zoom Range	4:1
Isotherm	10, 20, 50, 100, 200, 500, & 1500 Ranges
Field of View, typical	14° X 18° with 4:1 Zoom
Frame Rate	30 hz with 2:1 interlace
Spectral Range	8 to 12 microns
Detector	HgCdTe
Resolvable Elements per Line	>150
Lines per Frame	525 Raster, >200 IR
Focus Range	5" to Infinity
Detector Coolant	Liquid Nitrogen
Coolant Hold Time	>2 hours
Power Requirements	12 volt battery or 110v AC
IR Scanner Size (HxWxL)	5" X 4½" X 6½"
Control/Electronics Unit Size (HxWxL)	5½" X 8½" X 8½"
IR Scanner Weight	4 lbs.
Control/Electronics Weight	5½ lbs.

## ADDENDUM 1

### Thermal Suppression Requirements

#### 1.0 INTRODUCTION

The suppression requirements which have been generated and are presented in the following discussion are not intended to be final and general. Rather they were generated at the beginning of this project for the purpose of providing a guide or standard against which to measure the performance and adequacy of thermal camouflage-in particular that afforded by the perfusion screen. It was recognized during the development of the requirements that some areas of exploration into refining the requirements could not be pursued due to time and money limitations. Therefore the requirements are presented as proposed ones subject to modification. They are however, felt to be adequate to serve as the working definition of thermal requirements for evaluation of the perfusion screen.

The thermal camouflage requirements have been divided into three parts: the basic one of radiant emittance, thermal patterning and angular coverage. They will be discussed in that order.

#### 2.0 RADIANT EMITTANCE REQUIREMENT

Spectral radiant emittance from the scene is the fundamental parameter which controls what is imaged by a thermal imaging sensor. For the purposes here, the integrated radiant emittance within the sensor spectral operating region will be the term of interest. It is possible to represent this quantity with the equivalent blackbody temperature. The equivalent blackbody temperature of an object is just the blackbody temperature which would produce the same radiant emittance as that object. A brief consideration of the equivalent blackbody temperature is presented in the next section to show equivalency to radiant emittance.

## 2.1 Equivalent Blackbody Temperature as a Replacement For Radiant Emittance

This development presents the rationale for using equivalent blackbody temperature in place of radiant emittance in discussions of the camouflage thermal requirement.

If we define  $W_{12}(T)$  as the radiant emittance for an object at temperature,  $T$ , with emissivity  $\varepsilon(\lambda)$  in the wavelength band  $\lambda_1$  to  $\lambda_2$  then it is expressible in terms of the blackbody spectral radiant emittance,  $W_{b\lambda}(T)$ , as

$$W_{12} = \int_{\lambda_1}^{\lambda_2} \varepsilon(\lambda) W_{b\lambda}(T) d\lambda \quad (1)$$

This can be approximated as

$$W_{12} \approx \varepsilon_{avg} \int_{\lambda_1}^{\lambda_2} W_{b\lambda}(T) d\lambda \quad (2)$$

$$\text{where } \varepsilon_{avg} = \frac{1}{\lambda_2 - \lambda_1} \int_{\lambda_1}^{\lambda_2} \varepsilon(\lambda) d\lambda \quad (3)$$

Again it is possible to approximate the blackbody radiant emittance in the  $\lambda_1$  to  $\lambda_2$  waveband as the total blackbody radiant emittance times a factor representing the fraction within the waveband,

$$\int_{\lambda_1}^{\lambda_2} W_b(T) d\lambda = F(\lambda_1, \lambda_2, T) \sigma T^4 \quad (4)$$

where  $T$  = actual object temperature, K  
 $\sigma$  = Stefan Boltzman constant  
 $F(\lambda_1, \lambda_2, T)$  = fraction of total blackbody radiant emittance in the  $\lambda_1$  to  $\lambda_2$  waveband for temperature  $T$

Therefore the object radiant emittance in a given waveband can be expressed as

$$W_{12} = \epsilon_{avg} F(\lambda_1, \lambda_2, T) \sigma T^4 \quad (5)$$

The equivalent blackbody temperature is the blackbody temperature ( $\epsilon=1$ ) producing the same radiant emittance,

$$F(\lambda_1, \lambda_2, T_{bb}) \sigma T_{bb}^4 = \epsilon_{avg} F(\lambda_1, \lambda_2, T) \sigma T^4 \quad (6)$$

It may be shown that as long as  $\epsilon_{avg}$  is high, and the temperatures  $T_{bb}$  and  $T$  are not very different (less than 15°C),

$$F(\lambda_1, \lambda_2, T_{bb}) = F(\lambda_1, \lambda_2, T)$$

quite closely (less than 4% typically).

Thus

$$T_{bb}^4 \approx \epsilon_{avg} T^4 \quad (7)$$

and

$$T_{bb} \approx \sqrt[4]{\epsilon_{avg}} T \quad (8)$$

is the equivalent blackbody temperature.  $T_{bb}$  arrived at in this way gives a single number which is easily related to, yet characterizes the radiant emittance for an object.

It includes emissivity as well as actual temperature. Therefore, when two surfaces with different emissivities are compared in terms of actual and equivalent blackbody temperatures, the results may not agree closely.

The relationship between actual temperature differences and equivalent blackbody temperatures can be expressed from (A8) as

$$T_{bb^1} - T_{bb^2} = \sqrt[4]{\epsilon_1} T_1 - \sqrt[4]{\epsilon_2} T_2 \quad (9)$$

If the emissivities are different, the actual and equivalent blackbody temperature differences can vary considerably. For example, the table below lists actual temperatures and the corresponding equivalent blackbody temperatures and the delta Ts, for two surfaces.

<u>Surface</u>	<u>T<sub>actual</sub></u>	<u>ΔT<sub>actual</sub></u>	<u>ε</u>	<u>T<sub>bb</sub></u>	<u>ΔT<sub>bb</sub></u>
2	300K	> 16K	.98	298.5	> 9.3K
1	316K		.90	307.5	

The difference in emissivity from .9 to .98 results in about a seven degree variance between actual and equivalent blackbody temperature differences.

When the two emissivities are equal ( $\epsilon_1 = \epsilon_2 = \epsilon$ ) then the difference becomes just

$$T_{bb^1} - T_{bb^2} = \sqrt[4]{\epsilon} (T_1 - T_2) \quad (10)$$

and the differences between actual and equivalent blackbody temperature differences is negligible provided the emissivity is high (like 0.90).

## 2.2 Approach to Defining Temperature Requirements

Since the radiant emittance of an object (camouflage or background) is representable by its equivalent blackbody temperature, the camouflage requirement can be presented as a temperature limitation.

It has been found convenient to divide the temperature requirement into two cases depending on range from sensor to target. The range at which the target just fills the instantaneous field of view (IFOV) of the sensor is defined as the critical range,  $R_c$ .

The "resolved target" case corresponds to ranges shorter than  $R_c$  for which the target angular subtense is greater than the sensor IFOV. Then the "unresolved target" case corresponds to ranges greater than  $R_c$  for which the target angular subtense is less than the sensor IFOV. Unresolved targets are therefore of the "star" type - point sources.

One matter which should be addressed here is the meaning of the word "detection" in the present discussion. It is understood here to mean the perception of an object such that something about the object causes the observer to regard it with suspicion as unnatural or man-made. When an object is thus detected it comes under more concentrated scrutiny. This is to be distinguished from the instance of just being able to discern that something is different from its immediate background - i.e. just to "see" it or "detect" it in a strict sense. Other cues must also trigger the suspicion response, such as regular shape, movement, or significantly greater thermal contrast with the average background than is true for most objects in the background.

## 2.3 Suppression Requirement For the Resolved Target

Thermal sensors typically have minimum resolvable temperature differences on the order of tenths of a degree Centigrade. This means that scene objects which have temperatures different

from adjacent objects by as much as one degree can be differentiated from those objects by thermal sensors - "detected" in the strict sense. Since it is not realistic to require that camouflage blend thermally to one degree or less, it is accepted that the camouflage will in general appear in thermal images of scenes in which it is present. The requirement, therefore, centers on controlling those features about the camouflage which attract attention and cause an observer to have suspicions about its naturalness.

This step removes any relationship of the camouflage temperature requirement with sensor performance for the resolved target and ties the requirement directly to the background. As far as camouflage temperature is concerned then the basic criterion is that:

A camouflaged target must have equivalent blackbody temperatures which fall in the range of naturally occurring equivalent blackbody temperatures for the background in the vicinity of the target. More particularly, the camouflaged target should have temperatures in the range of those for similarly shaped areas of the background.

The latter sentence just means that if the camouflage target has the roundish outline of a tree as seen from above, it should have temperatures associated with trees in the background and not those for rocks or bare soil areas of a different shape from the camouflage.

This criterion is fundamental, but not quantitative for a given season or time of day. It is desired that more quan-

titative limitations be found as a guide. This was sought in data for background temperature variation. A reference point from which to measure specific variation in background temperature is average background temperature. The quantitative guide for resolved target camouflage is proposed in terms of a limitation on the difference between camouflage and average background equivalent blackbody temperatures.

It is convenient to note that air temperature can be used as an estimate of average actual background temperature. In the day, transpiration holds foliage temperature at or below air temperature, while other objects rise above air temperature due to solar loading. At night, residual solar heat release may make some objects remain above air temperature while radiation to the cold sky causes other objects to fall below air temperature. Thus air temperature lies at an intermediate point between the extremes of temperature in the background. Link, in Reference 1, supports this when he says that air temperature is the "single most important parameter" for predicting background temperature. It is one simply measured temperature which immediately produces an estimate of average background temperature.

The approach to establishing quantitative limits for camouflage temperature variation from average background was to locate equivalent blackbody temperature variations in typical backgrounds, or lacking that, to use actual background variations from air temperature and neglect the difference between those and equivalent blackbody temperature variations because it is understood that the quantitative results will in any case only be an estimate of the actual requirement. Since natural objects generally have high emissivities, actual = equivalent blackbody estimate is not too bad though in a more exact determination this should be taken into account.

An attempt was made to organize the limited amount of data found into conditions with similar differences with air temperature. The categories of bright sun, early evening or day heavy overcast, and pre-dawn were selected.

#### Bright Sun

The temperature difference between leaves and air in mid-day sunlight is up to 20 deg C (Ref. 2, p. 276). In moderate sun (about  $60 \text{ mw/cm}^2$ ), dry soil will have equivalent blackbody temperature about 20 deg. C warmer than plant leaves or perhaps 30 deg. C. warmer than air (Ref. 2, p. 282). The moisture condition of the soil also influences plant leaf temperatures in the sun. Reference 3 shows that well watered plants have leaf temperatures below air temperature. Squash plants shown there varied from 4 to 8 deg. C cooler than air during a diurnal cycle. Other crop foliage temperatures also remained at or below air temperature for tests in North Dakota, Kansas, Nebraska, and Minnesota in the summer.

Equivalent blackbody temperatures were also measured with a handheld radiometric thermometer (Raytek R2LT) for various background objects (grass, trees, dry soil, plants) at Garland, Texas in November, 1981 to obtain a sample of afternoon temperature variation in bright sun. Objects naturally in the background (foliage and soil) measured from -1 to +15 deg. C relative to air temperature (soil at the upper end).

#### Early Evening

For the early evening hours Ref. 2, p. 291 has a figure with temperatures at 7:00 p.m. derived from infrared imagery (equivalent blackbody temperatures) which vary from 19 deg. C to 35 deg. C ( $16^\circ \text{ C}$  variation).

### Pre-Dawn

Early morning pre-dawn data on temperature was found in tests conducted in September, 1970 at Fort Huachuca, Arizona about 04:40. Actual contact temperatures on materials there on two mornings fell within  $\pm 2$  deg. C of air temperature. Another early morning test (temperatures measured between 04:00 and 05:00, 5/5/71) showed temperatures varying only  $\pm 1$  deg. C from air temperature.

Taking the above rather sparse data and using some judgement, the following set of equivalent blackbody temperature guidelines for camouflage are proposed for three conditions (with  $\Delta T = T - T_{\text{avg background}}$ ) in Table 1.

Table 1. Thermal Suppression Guidelines for Temperature

<u>Condition</u>	<u><math>\Delta T</math></u>
Bright Sun	$\pm 7^\circ$ C
Early Evening or Day Heavy Overcast	$\pm 4^\circ$ C
Pre-dawn	$\pm 2^\circ$ C

These temperature differences should be regarded in a "rule-of-thumb" fashion because of the wide variability of the background temperatures with insolation, wind, moisture, and type of background. The more correct requirement is still the basic one of remaining within the thermal variation of the background in the immediate vicinity of a camouflaged target as stated earlier.

## 2.4 Suppression Requirement for the Unresolved Target

Now for targets situated at ranges greater than the critical range, the target is unresolved (becomes a point source). What will be developed here is a set of curves representing the equivalent blackbody temperature difference between a camouflaged target and the average background corresponding to a 50% probability of detection as a function of range beyond the critical range (where the target becomes a point source). They are sample curves for two representative target sizes and two postulated threat systems. The temperature difference variation with range indicates the threshold at which a viewer sees the target half the time.

### Thermal Suppression Model

For the unresolved target suppression requirement model, the critical range,  $R_c$ , is defined as the range at which the angle subtended by the target is equal to the threat system IFOV:

$$R_c = w / \text{IFOV} \quad (11)$$

where

w = target dimension [m]

IFOV = threat system IFOV [rad]

For the purpose of this work, it is assumed that the vertical and horizontal IFOV's are equal and that the target is square.

At the critical range, a critical temperature,  $T_c$ , can be defined such that a target at this equivalent blackbody temperature can be detected with a specified probability. Using the small signal approximation  $T_c$  is given by

$$T_c = \text{SNR} \cdot \text{NETD} \cdot e^{\alpha R_c} + T_{bk} \quad (12)$$

where

$T_{bk}$  = equivalent blackbody background temperature [K]  
 $SNR$  = signal to noise ratio required for a specified target detection probability ( $P$ )  
 $\alpha$  = atmospheric attenuation coefficient [ $km^{-1}$ ]  
NETD = noise equivalent temperature difference of threat system [K]

SNR for use in (12) was chosen to be that for 50% probability of detection. That seems to be a proper threshold to define the camouflage requirement. The method of determining this SNR was to use the data tabulated by Rosell which appears in the NVI model for thermal viewing systems (Ref. 4, p. 20, Table 6) which was assumed to apply in this case, too. That 50% probability SNR from the table is 2.8.

This value is thought to be conservative (on the low side) in this application for a number of reasons. The test situation yielding data on which the SNR/probability relationship was based involved several factors tending to permit detection at lower SNRs than would be expected in the present application. They are (see Ref. 5):

- 1) resolved targets were used
- 2) no search process was involved, the observer knew that the target was in the center of the field-of-view.
- 3) the observer had unlimited viewing time for target detection.

In order to calculate  $R_c$  and  $T_c$ , it is assumed that

$w$  = 1 m and 2.3 m  
 $\alpha$  = 0.1  $km^{-1}$   
 $T_{bk}$  = 300K

The 2.3 meter width is the standard NATO target size and the 1 meter width corresponds to an estimate of heated area for typical engine driven electrical generators.  $R_c$  in equation (11) depends on threat system IFOV and  $T_c$  in (2) depends on NETD. These two threat system critical parameters were assumed as follows for two systems:

	IFOV [mrad]	NETD [°C]
Threat System A	0.5	0.2
Threat System B	0.1	0.1

Using Eq. (11) and Eq. (12), the following thermal suppression model parameters are evaluated:

	$R_c$ [km]	$T_c$ [K]	Target Size [m <sup>2</sup> ]
Threat System A	2.0	300.68	1 x 1
	4.6	300.89	2.3 x 2.3
Threat System B	10.0	300.76	1 x 1
	23.0	302.79	2.3 x 2.3

For a target at  $T_c$ , the radiant emittance within a wavelength interval from  $\lambda_1$  to  $\lambda_2$ ,  $W_{12}(T_c)$ , exceeds the background radiant emittance,  $W_{12}(T_{bk})$ , by

$$\Delta W_{12}(T_{c_1} T_{bk}) \equiv W_{12}(T_c) - W_{12}(T_{bk}) \quad (13)$$

For an unresolved target which is at a range  $R$  greater than  $R_c$ ,  $\Delta W_{12}(T_c, T_{bk})$  must be increased by a range factor in order to maintain the 50% detection probability SNR - i.e. to maintain the irradiance of the threat system as at  $R_c$ . This means that the further the range, the hotter the target can become to give the same probability of detection (SNR). It may be shown that the radiant emittance from target and background within the IFOV in order to maintain this condition is given by

$$W_{12}(T_{bb}) = \Delta W_{12}(T_c, T_{bk})(R/R_c)^2 \exp[\alpha(R-R_c)] + W_{12}(T_{bk}) \quad (14)$$

where  $T_{bb}$  = the equivalent blackbody temperature of the target

Note that when the target is at a range where it does not fill the entire IFOV, then the radiant emittance within the IFOV is due to background plus target. This results in an apparent temperature (equal to  $T_c$ ) which is less than the effective blackbody temperature of the target,  $T_{bb}$ .

Eq. (4) is the expression for the radiant emittance of the target at  $T_{bb}$  such that the detection probability is the same at any range  $R \geq R_c$ . By evaluating  $W_{12}(T_{bb})$  versus range, target temperature,  $T_{bb}$ , can be determined as a function of range. Figures 1 and 2 present plots of  $T_{bb} - T_{bk}$  versus target detection range for the postulated threat systems A and B, respectively, for two target sizes. Radiant emittances,  $W_{12}(T)$ , were calculated for  $\lambda_1 = 8\mu$  and  $\lambda_2 = 14\mu$  using a TI-59 calculator program written at Varo solving equation (14).  $T_{bb}$  was determined from calculated  $W_{12}(T_{bb})$  values using an iterative program method written for the TI-59 calculator.

**Figure 1**  
**Threat System A**

**T<sub>bb</sub>** = Equivalent Blackbody Temperature of Target  
**T<sub>bk</sub>** = Equivalent Blackbody Temperature of Background

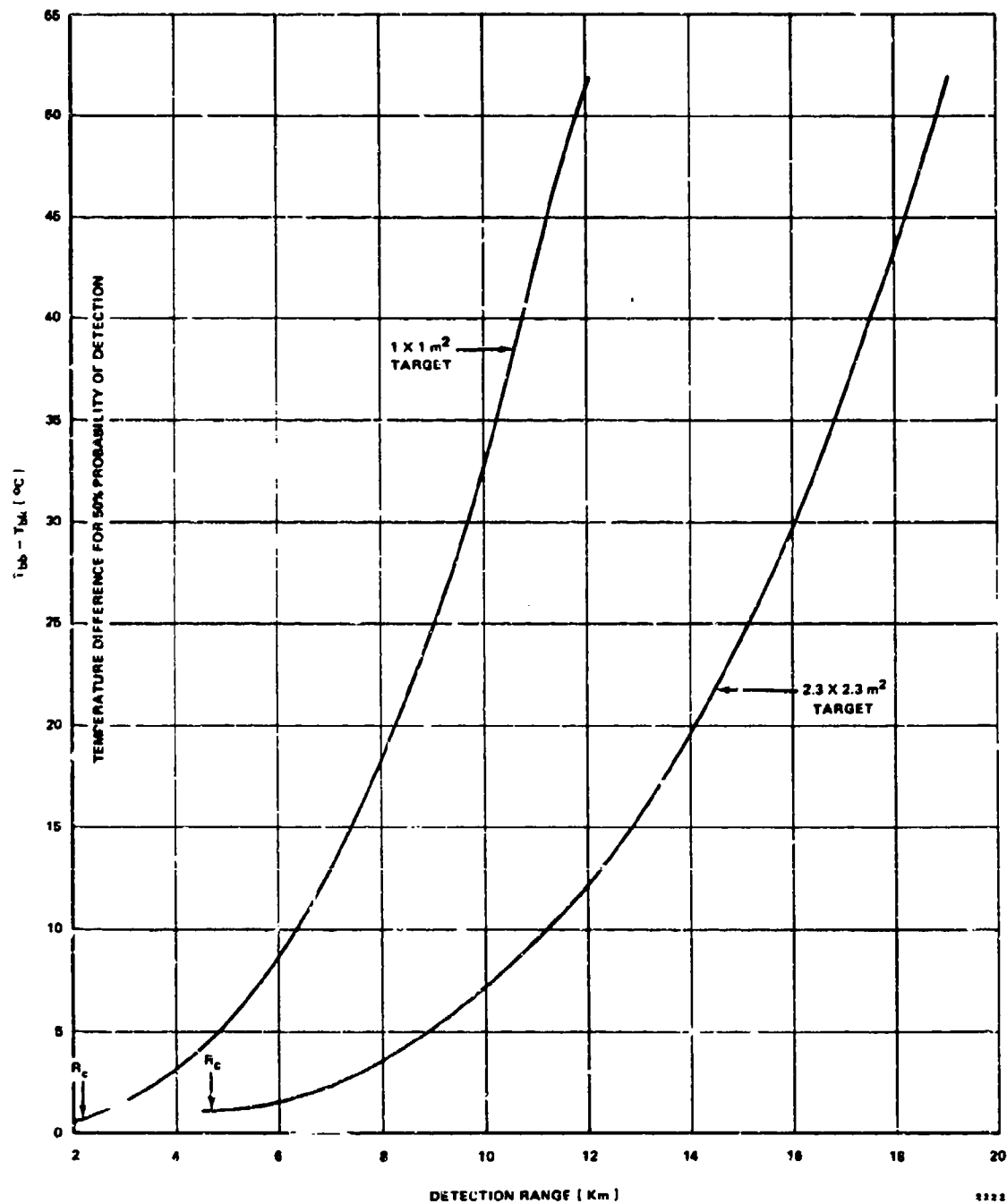
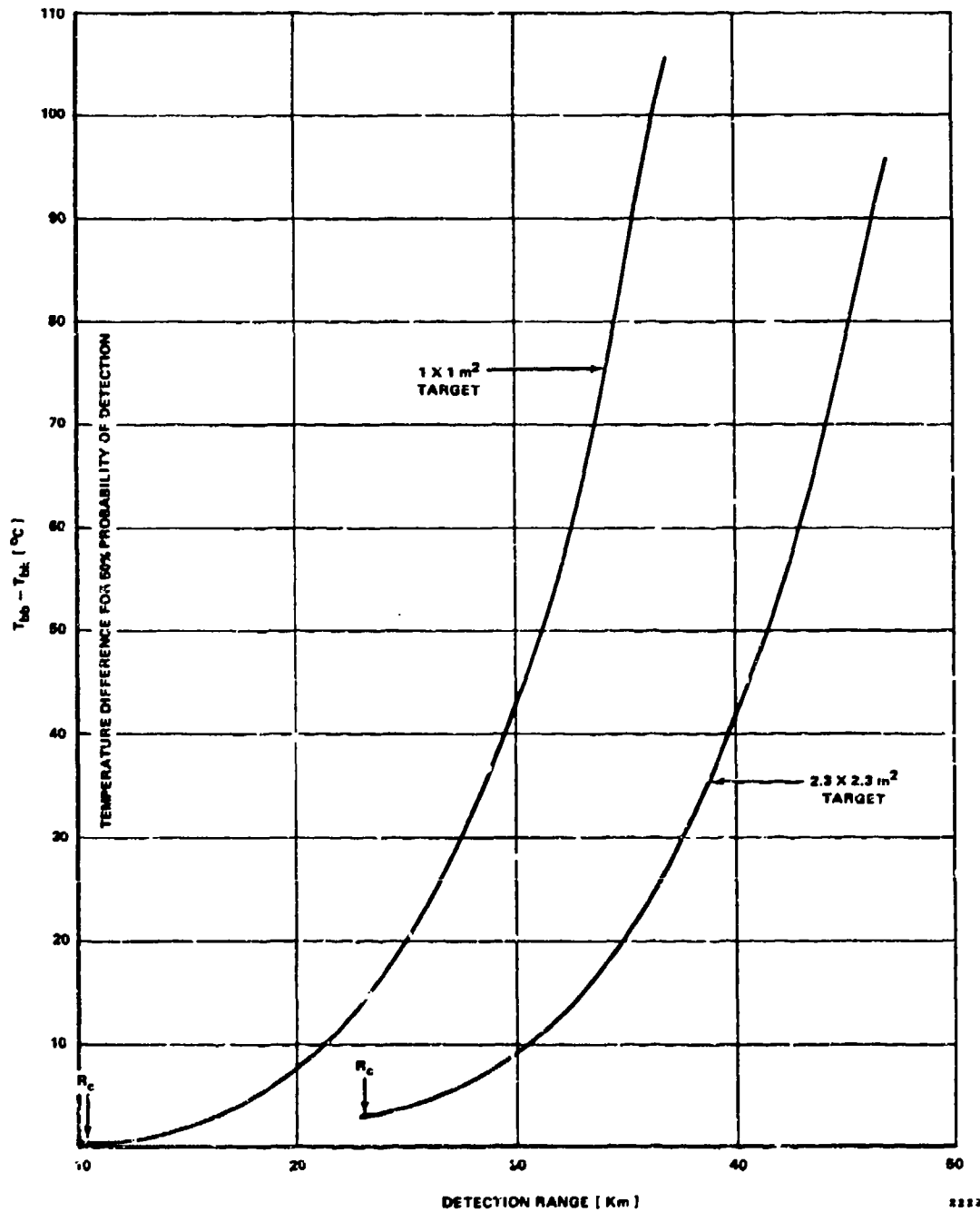


**Figure 2**  
**Threat System B**  
 **$T_{bb}$  = Equivalent Blackbody Temperature of Target**  
 **$T_{bk}$  = Equivalent Blackbody Temperature of Background**



The results in Figures 1 and 2 are plotted for a 50% probability of target detection. Each curve starts at the critical range where the target fills the IFOV of the threat system. Points along each curve represent the effective blackbody target temperature difference with background temperature, for threshold detection (50% probability) at the corresponding range. By using thermal camouflage to reduce target temperature difference with background, detection range is reduced. Ideally the camouflaged target temperature difference should be reduced to a point which we call the "clutter threshold". A working definition for the clutter threshold is the maximum positive and negative equivalent blackbody temperature difference with average background which is present in a given scene. The negative difference is also significant because targets are essentially equally detectable if they are equally colder or hotter than the background.

The environmental conditions discussed in Table 1 of Section 2.3 indicate that the clutter threshold may vary from two to seven degrees above or below average background. Once the apparent target temperature difference with ambient is reduced to the clutter threshold using camouflage, the unresolved target has the same detection probability as other objects in the scene at the clutter threshold temperature. Therefore, the thermal suppression goal for the unresolved target is to reduce the apparent target temperature difference with average background temperature to the clutter threshold or below. For a clutter threshold temperature less than the critical temperature, the thermal suppression requirement is that the camouflaged target temperature difference with average background be at or below the critical temperature. The latter case is expected to be rare.

By scaling off Figure 7 of that MIL spec, it is possible to get the dimensions of smaller pattern lobes. A sample of dimensions so measured are (in inches): 18, 15, 16, 30, 14, 8, 8, 8, 13, for an average of about 14 inches.

According to the Guide to Camouflage for DARCOM Equipment Developers (29 April, 1978) page 36, the human eye has an angular resolution of about 0.3 - 0.9 mr. Attempting to make a generalization from this take the ratio of lobe dimension to eye resolution (using an average of 0.6 mr),

$$\frac{\text{lobe dim}}{\text{eye res.}} = 14''/0.6 \text{ mr} = 23''/\text{mr}$$

That however, leads to a criterion of lobe dimension for a tenth mr resolution thermal imager of 2-3 inches. That seems excessively small from a common sense viewpoint.

There are perhaps two factors which would indicate a larger pattern size for the thermal region. First is the range at which eyes operate vs. the normal range for a thermal imager. Patterning for the eye at 300 meters is one thing but patterning for an imager at 1000m should be another. That may suggest a factor of three increase in thermal lobe size beyond the 23"/mr visual criterion. Secondly, the richness of contrast and colors available to the eye in a visual scene is a force toward greater patterning for visual camouflage. In the thermal imaging system, however, there is ordinarily a monochrome display and therefore less information than typically available in a visual display. Subjectively that may be assessed as another factor of two toward relaxing the size of thermal patterning to bigger sizes.

### Overall Temperature Requirement

Combining both the resolved and the unresolved target cases it can be said that a general requirement is that the camouflaged target equivalent blackbody temperature difference with that of the average background be in the range indicated in Table 1 - within two to seven degrees C of the average background depending on environmental conditions.

It should be pointed out that camouflage measures which do not succeed in achieving those difference levels are not necessarily of no utility, because any reduction in temperature results in a reduced detection range which is of some benefit. If camouflage measure-of-effectiveness is some function of detection range reduction due to camouflage, then particularly at longer ranges, Figures 1 and 2 provide a framework in which to evaluate that measure-of-effectiveness.

### 3.0 THERMAL PATTERN DISRUPTION

Assuming that the thermal camouflage measures applied to a particular target have brought its overall temperatures into the range of those in the background, there remains the problem of shape and pattern. Though the target may have equivalent blackbody temperatures which fall in the range of those in the background, the target may be square or have a uniform temperature across its extent whereas nothing in the background looks like that to the observer. Thus it attracts his attention and is detected. This is just to say that more than temperature control is necessary to avoid detection in the resolved case. For unresolved targets of course, patterning on the target is not at all a factor.

One source of information about patterning of camouflage is visual camouflage. Visual patterning is described in Mil-C-52771A (ME) 23 February, 1976, for the lightweight synthetic camouflage s a.

Considering a ground imager operating at a range of 1000 meters with a resolution of 0.2 mr, the lobe dimension for camouflage would be (using the visual criterion of 23"/mr moderated with the factor of six for range and color difference between visual and thermal)  $23'' \times 0.2 \times 6 = 27$  inches.

Another estimate can be arrived at by considering a 0.1 mr thermal imager operating at a range of 1500 meters aerial. That suggests a range of  $(1500/300) \times 2 \times 23$  inches/mr  $\times (0.1\text{ mr}) = 23$  inches.

Some examples of good nighttime thermal imaging were also examined to note the apparent sizes of background patterns. A thermal picture of a wooded area (Chambers Brother's Sand in Garland, Texas) taken with an RS310D on 8/76 shows lobes in trees and bushes which are about 14 inches (taking the width of a trailer bed in the image as eight feet and scaling other features). Another thermal image in the winter, this time at Fort Sill, OK, with the same imaging system shows details in the tree limbs which scale in a similar way to about 17 inches.

Taking an average of all of the above estimates get lobe dimension as

$$(14 + 17 + 27 + 23)/4 = 20 \text{ inches}$$

Therefore, it is proposed that the size of lobes in camouflage pattern for the thermal perfusion screen should be about 20 inches. Larger sections would of course be put together in patterning but the smaller lobes should be on the order of 20 inches.

One observation on patterning which stems from examination of the thermal imagery from Chambers Sand and Fort Sill taken with the RS310D sensor system is that the patterns in a foliated background condition are associated with trees and bushes macroscopically. The whole tree forms a roundish pattern. Grassy background makes a more uniform thermal radiance area with less contrast. However, in the winter imagery, trees have a distinct warm pattern at night when the major limbs are resolved. Radial lines then form a network emanating from the center except in cases in which the sensor was looking forward when the tree is seen from an oblique view, rather than strictly from the top. It is probable that an attempt to create that sort of pattern thermally with a screen will be quite difficult. The winter condition in a wooded area may present special difficulties when the target is resolved.

#### 4.0 ANGULAR COVERAGE REQUIREMENT

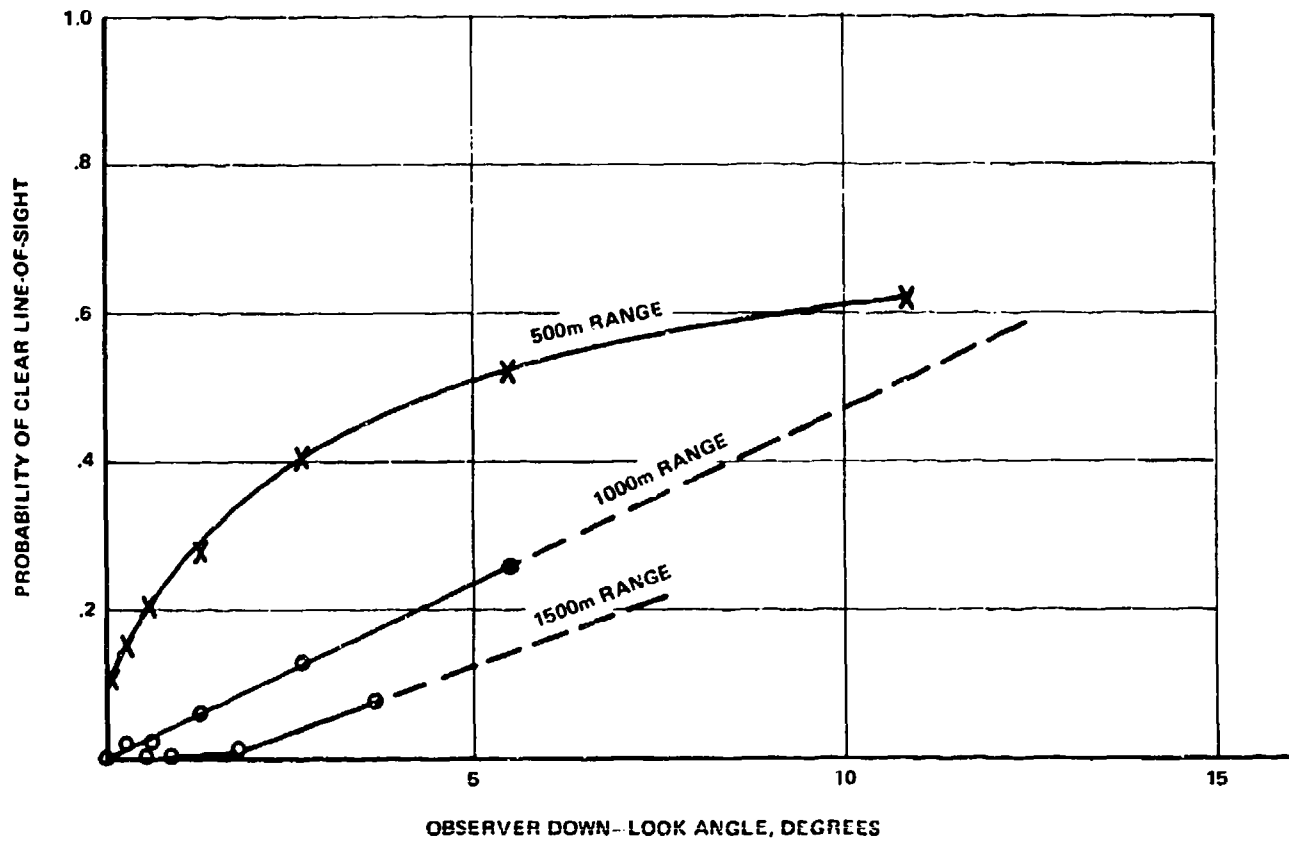
This section addresses the problem of defining the angular coverage of a target which thermal camouflage needs to provide in order to adequately hide.

Thermal viewers of different types taken as a set are capable of observing a target from all angles in a hemisphere. Sensor systems operating from a ground position present the potential of viewing the camouflaged target along horizontal lines-of-sight while airborne and satellite sensors can operate at all other angles. Therefore, from this consideration alone, camouflage in the thermal spectrum needs to offer full hemispheric coverage (all azimuth angles and from 0 to 90 degrees from the vertical in elevation).

However, in many geographic areas, terrain masking alleviates that requirement. That is to say, if terrain features are interposed between the sensor and the camouflaged target for some angles of view, then those angles of view need not be covered by the camouflage.

In an attempt to examine terrain masking, a curve (Fig. 6-11) in reference 6 on terrain masking at various ranges and observer heights, was used. It gives the probability of clear line-of-sight from the observer position at different heights above the target as a function of range from observer to target at Grafenwaehr, Germany. This is taken to be representative of terrains of interest. The target was a 7 foot rod (top of the rod assumed to be the actual point sighted on). This data was replotted to give the probability of a clear line-of-sight for a constant range as a function of elevation angle above the horizontal (Figure 3). It suggests that as observation range gets smaller the probability of clear line-of-sight improves for the same observation angle. That probably reflects the diminished likelihood of having masking features on a given line-of-sight as the range is decreased. (Density of trees and hills is a constant so one expects fewer of them on a shorter line segment).

It is thought that a 1000 meter range criterion for thermal camouflage is reasonable for requiring angular concealment performance. If that is acceptable, then an angular coverage down to five degrees of the horizontal would offer a probability of masking ( $1 - \text{clear LOS probability}$ ) of about .75 from Figure 3. If, however, the range must be as close as 500m to the camouflaged target from the observer sensor thermal system, then the coverage has to go essentially to the ground (90 degrees from vertical) because masking may not be relied upon to afford much protection. For 75% probability of masking the figure suggests the angle would have to be about one degree above the horizontal - corresponding to virtually hemispheric coverage.



2224

Figure 3. Data From Figure 6-11 Replotted, Grafenwoehr Probability of Clear Line-of-Sight From Observer to 7 Foot Rod

It can be observed in addition that azimuthal considerations might make it desirable to execute a full to-the-ground coverage for most azimuth angles, but relax the elevation coverage at one or two angles (of azimuth) pointing away from the FEBA where less risk of observation may be anticipated.

## 5.0 REQUIREMENTS SUMMARY

The integrated results of the foregoing analysis is presented here. Although it is qualitative, the most exact thermal requirement for camouflage is that the equivalent blackbody temperature of the camouflage fall within the naturally occurring range of the background. That holds generally true both for cases in which the target is resolved (several resolution elements across the target) and for the unresolved target case (point sources). In the latter case the analysis shows that this may be too restrictive, but the camouflager cannot be expected to know how far away the threat sensor will be and so must treat for the worst case.

It is proposed quantitatively that camouflage equivalent blackbody temperatures need to be within from  $\pm 2$  to  $\pm 7^{\circ}\text{C}$  of average background temperature, depending on the environmental condition. These kind of numbers are to be taken only as guidance - not absolute requirements - because of the variability of the background for different environments and location.

It is interesting to note that the unresolved target analysis points out the possibility of achieving long range detection avoidance without the necessity of reducing target temperatures as low as the background temperatures.

The result of pattern analysis was that thermal patterning should be on the order of 20 inches (for the smallest lobes in an irregular pattern.

Angular coverage analysis suggests that terrain masking effects may permit some relaxation from a full hemispheric coverage requirement. A one to five degree region above the horizontal may be frequently masked by terrain so that angular region does not have to be covered by camouflage.

## REFERENCES

1. Link, L. E., Terrain thermal modeling for camouflage and terrain acquisition, 6/1980. U. S. Army Engineer Waterways Experiment Station, Vicksburg, Mississippi
2. Shay, J. R., Remote Sensing, National Academy of Sciences, Washington, D. C., 1970
3. Idso, S. B., R. D. Jackson, P. J. Pinter, Jr., R. J. Reginato and J. L. Hatfield, 1981. Normalizing the stress-degree-day parameter for environment variability. Agric. Meterol. 24:45-55.
4. J. A. Ratches, R. J. Bergemann, W. R. Lawson, T. W. Cassidy, L. P. Obert, J. M. Swenson, April 1975. Night Vision Laboratory Static Performance Model for Thermal Viewing Systems. U. S. Army Electronics Command Report ECOM-7043
5. J. A. Ratches, Static performance model for thermal imaging systems. May, 1976. Opt. Engr. V.15, No. 6
6. L. P. Obert, J. T. Wood, G. J. Nash, Visionics EO, Sensor Performance Handbook (U), Vol I, Natural European Environment, June, 1981. USA MERADCOM Night Vision and Electro-Optics Laboratory report by DCS Corp., Arlington, VA.

## THERMAL LOAD FOR CAMOUFLAGE

A measure of the thermal perceptibility of a target is the difference in radiant emittance between the target and the ambient. That is translatable to a difference in equivalent blackbody temperatures. Reducing target surface temperature difference with ambient is a characterization of the thermal camouflage task.

Another way to view thermal load is that of the influence of targets on the temperature of camouflage material. Again, that basically results from temperature differences of the target with its ambient, although that is affected by environmental factors and the mode of camouflage application to the target.

Thermal load coming from these two viewpoints thus centers on target surface temperature differences with ambient. The approach taken here was to search out these differences for a few typical targets which were assumed to be representative of targets in general. The targets selected were engine driven electrical generators and a tank.

A particularly useful set of data on a tank (German Leopard 1) is found in Reference 1. Temperatures were deduced from AGA 680LW thermal pictures operating in the 8-14μm region. Temperatures are, therefore, apparently equivalent blackbody temperatures.

The conclusion was reached that 98% of all pixels from the picture of a moving Leopard tank in the day were from about -1 to 42°C warmer than average background (taken to be 13°C from air temperatures given). That gives a crude average difference with background of 21°C. Not much of the tank was more than 40°C warmer than the background (only 5%). Data from past experiments by Varc on diesel driven electric generators shows the maximum difference with ambient temperature for non-exhaust surfaces was about 30°C (radiator). For skin temperature on top near the muffler, the maximum difference with ambient was about 25°C. Those were nighttime temperatures.

Data on tank temperature differences due to solar load can be obtained from Reference 2, Appendix A. Those data show that objects like the toolbox which have little thermal mass actually heat up worst of all, exhibiting temperatures in the sun about 33°C warmer than air. Armor surfaces showed temperatures about 15 to 20°C warmer than air.

Combining the above data together, it is proposed that a generalized target with the following maximum surface temperature differences with ambient be used for a working definition of thermal load:

Daytime	30-40°C
Night	25-30°C

## REFERENCES

1. A. Assfalg, K. Klodt, R. Schmidt, J. Vogtenrath, Measurement of ir signatures of ground vehicles. June, 1979. Proc. KRC Symposium on Ground Vehicle Signature, Vol. 1, Keweenaw Research Center, Houghton, MI
2. J. H. Hopkins, D. L. Gee. Evaluation of solar heat reflecting paints for reducing thermal stress. Jan. 1967., Report 1886, U. S. Army Engineer Research and Development Laboratories, Fort Belvoir, Virginia 22060.

DISTRIBUTION LIST

<u>Addressee</u>	<u>Copies</u>
Commander U.S. Army Mobility Equipment Research and Development Center Fort Belvoir, Virginia 22060	
Attn: DRDME-RT DRDME-WC	20 2
Defense Technical Information Center	2
Attn: DTIC-M Cameron Station Alexandria, Virginia 22314	